Supporting information for

Mutations in *CLCN6* as a novel genetic cause of neuronal ceroid lipofuscinosis

by Hailan He, Xiaoshuang Cao, Fang He, Wen Zhang, Xiaole Wang, Pan Peng, Changning Xie, Fei Yin, Dengfeng Li, Jiada Li, Minghui Wang, Malte Klüssendorf, Thomas J. Jentsch, Tobias Stauber*, Jing Peng*

*To whom correspondence should be addressed:

tobias.stauber@medicalschool-hamburg.de (T.S.), pengjing627@126.com (J.P.)

Contents:

Material and methods

Antibodies

Primary antibodies were rabbit against SQSTM1/P62 (Cell Signaling Technology), rabbit against LC3 (Cell Signaling Technology), and mouse against β-actin (Sigma), rabbit anti-IBA-1 (Wako), rat anti-Lamp-1 (BD Pharmingen), rabbit anti-GFAP (Cell Signaling Technology), rabbit anti-cathepsin D (Abcam), rabbit anti-cleaved caspase-3 (Cell Signaling Technology), rabbit anti-phos-p70 S6 kinase (Cell Signaling Technology), mouse anti-p70 S6- kinase (Santa Cruz), rabbit anti-mTOR (Cell Signaling Technology), mouse anti-calbindin (Sigma), rabbit anti-somatostatin (BMA Biomedicals), mouse anti-parvalbumin (Sigma), rabbit anti-calretinin (Cell Signaling Technology), rabbit anti-ATP synthase subunit c (a gift from Eiki Kominami, Juntendo University, Tokyo, Japan)[1], rabbit anti-ClC-3[2], rabbit anti-ClC-4[3], rabbit anti-ClC-6 (6C3)[4] and rabbit anti-ClC-7 (7N4B)[5]. Secondary antibodies coupled to Alexa Fluor 488 or 546 were obtained from Thermo Fisher Scientific.

Cell cultures, plasmids and transfection

Human cervical adenocarcinoma cells (HeLa) were cultured at 37 °C with 5 % CO2 in high glucose Dulbecco's modified Eagle medium, supplemented with 10 % fetal bovine serum, penicillin (100 U/mL), streptomycin (100 μg/mL). N-terminally GFP-tagged ClC-6 and N-terminally mCherry-tagged ClC-6 were as previously described[6, 7]. The ClC-6 p.E200A or ClC-6 p.Y553C constructs were generated by site-directed mutagenesis using the QuikChange site-directed Mutagenesis Kit (La Jolla, USA). All constructs were verified by sequencing of the complete open reading frame. The expression plasmids encoding either human WT ClC-6, ClC-6 p.E200A, p.E267A or p.Y553C were transfected alone or together with TFEB-eGFP or TFE3-eGFP plasmids into HeLa cells using LipoMax (SUDGEN) or FuGENE 6 (Promega) transfection reagent following the manufacturer's instructions. For co-expression, constructs were co-transfected at equimolar ratios. Each experiment was repeated at least three times.

Generation of *Clcn6*$^{E200A/+}$ knock-in mice and *Clcn6*-knockout mice

Mice were housed in the Central South University genetic animal facility or Delbrück-Centrum für Molekulare Medizin animal facility (approved by and in compliance with local authorities, LAGeSo Berlin, Germany) at 24-26 °C, with 50 % humidity, under 12-h light/12-h dark cycles, with free access to food and water. Mice were housed in the Central South University genetic animal facility or Delbrück-Centrum für Molekulare Medizin animal facility (approved by and in compliance with local authorities, LAGeSo Berlin, Germany) at 24-26 °C, with 50 % humidity, under 12-h light/12-h dark cycles, with free access to food and water. Mice were housed in the Central South University genetic animal facility or Delbrück-Centrum für Molekulare Medizin animal facility (approved by and in compliance with local authorities, LAGeSo Berlin, Germany) at 24-26 °C, with 50 % humidity, under 12-h light/12-h dark cycles, with free access to food and water. Mice used in this study were C57BL/6J strain. *Clcn6*$^{E200A/+}$ knock-in mice and *Clcn6*-knockout mice were generated by the Nanjing Biomedical Research Institute using CRISPR/Cas9 genome-editing technology. Embryonic stem cells were obtained from C57BL/6J mice. The single-guide RNA (sgRNA, GAAGGCCCCATGATCCACAG) targeting within exon eight of the *Clcn6* gene was used for embryo injection together with CRISPR-associated nuclease 9 (Cas9) and a single-stranded DNA oligonucleotide with a GAA codon (coding Glu200) mutated to GCA (coding Ala) as repair template. In addition to these planned knock-in mice, CRISPR also generated a 2-bp deletion in exon eight. The caused reading frame shift resulted in a TAG stop codon in exon eight and truncation of ClC-6 in a newly generated *Clcn6*-knockout (*Clcn6*$^{-/-}$) mouse line. Chimeric founder (F0) mice were selected and confirmed by PCR and DNA

sequencing. However, attempts to generate F1 offspring by mating heterozygous F0 *Clcn6*$^{E200A/+}$ mice with C57BL/6J mice failed. For the subsequent generation of mice, male *Clcn6*$^{E200A/+}$ were used as sperm donors for in vitro fertilization. Male and female F1 heterozygous *Clcn6*$^{+/-}$ mice were mated to generate homozygous *Clcn6*$^{-/-}$ mice. The genotypes of *Clcn6*$^{E200A/+}$, *Clcn6*$^{-/-}$ and wildtype (WT) littermates were confirmed by sequencing of the genomic DNA from tail biopsies.

In vivo structural MRI

In vivo MRI was performed on a 3-Tesla MRI scanner (Siemens, Germany). Mice were anesthetized with isoflurane with oxygen and air, then placed on a 37 °C heated bed. After anaesthesia, axial T2-weighted images (repetition time = 350 ms, echo time = 11 ms, slice thickness = 2.0 mm and field of view= 64×64 cm) were acquired. Ten animals (3 WT, 4 *Clcn6*$^{E200A/+}$, and 3 *Clcn6*$^{-/-}$ mice) were imaged at 5 months of age.

Video EEG recordings

For video EEG recordings, mice (n = 4 per genotype) were mounted in a stereotaxic frame and surgically implanted with EEG wireless telemetry transmitters (PhysioTel™ HD-X02-DSI) under 2-3 % isoflurane inhalation anesthesia. Briefly, two small holes (1 mm diameter) were drilled in the skull, then two electrodes were inserted and placed on the left and right hemispheres of the animals (-2 mm posterior to bregma and ±2 mm lateral to the midline). Electrodes were secured with dental cement and EEG telemetry transmitters were implanted in a subcutaneous pocket prepared in the hindermost dorsal region of the animal. Mice were then individually housed in a 12-h light/12-h dark, temperature- and humidity-controlled transparent cages with free access to food and water. Seven days after surgery, continuous one-channel video-EEGs were recorded in freely moving mice for at least 48 h using an in vivo EEG monitoring system (DSI's Physiotel Digital system). Data were analyzed by a visual inspection of the EEG using the Neuroscore software.

Electroretinogram recordings

For Electroretinogram (ERG) recordings (Roland Consult, Germany), mice were dark adapted for at least 4 h and anesthetized with intraperitoneal injection of 2 % pentobarbital sodium. Pupils were dilated with one drop of 2.5 % phenylephrine and 2.5 % tropicamide, and the cornea was anesthetized with 1 % proparacaine. Mice were then positioned on a heated platform and contact lens recording electrodes were placed on corneas of both eyes, with a ground electrode inserted subcutaneously between both eyes, and a reference electrode was introduced subcutaneously in the tail. All procedures were performed under dim red light. Scotopic ERGs were recorded by

a series of flashes with intensity of 0.01-10 cd.s/m^2 on a dark background and averaged. Rod responses were then saturated by a bright background for 5 min. Photopic responses were recorded by a series of flashes with intensity of 3-30 cd.s/m^2 on a light background.

Behavioral tests

Clcn6$^{E200A/+}$, *Clcn6*$^{-/-}$ and WT mice were evaluated in a battery of behavioral tests at different time points (1, 3 and 5 months of age). All behavioral tests were performed in the same room after at least 30 min of acclimatization.

Rotarod test

Motor coordination and balance was assessed using Rotarod. Each mouse was trained three times per day at 30-min intervals for three consecutive days. On day 1, mice were trained at a constant speed of 5 rpm. On day 2, mice were trained at a constant speed of 10 rpm. On day 3, mice were trained at a constant speed of 15 rpm. Mice were then tested on the rod at a fixed speed of 20 rpm for 3 trials with a 30-min break between each trial on day 4. The latency to fall off the rod was recorded for each mouse over a maximum observation period of 5 min, and the mean latency to fall off the rotarod of 3 trials was used for statistical analysis.

Beam balance test

Mice were trained to traverse a square, 12-mm-wide, 60-cm-long horizontal wooden bar toward a dark escape box at least 3 consecutive days with three trials per day. Latency to traverse the beam and number of times the hind feet slip off the beam were recorded over a maximum period of 60s, and three trials were performed.

Footprint test

Footprint test was performed to assess gait characteristics as previously described[8]. The forelimbs and hindlimbs of each mouse were coated with red and black non-toxic paints, respectively. Mice were required to walk along a straight narrow tunnel (20 cm X100 cm X50 cm) with an 80-cm long sheet of white paper on the floor to record the prints. A sequence of five consecutive steps was chosen for analysis, excluding footprints made at the beginning and at the end of the run. Font base width, hind base width, forelimb stride length, hind-limb stride length, overlap between hind and forelimbs were recorded.

Hanging wire test

Neuromuscular abilities and muscle strength were tested with the hanging wire test. Mice were placed on the top of a wire cage lid. The lid was gently shaken three times to improve the grip of mice, then turned upside down 50 cm elevated above a surface with bedding. The latency to fall from the wire lid was recorded over a maximum

period of 60 s.

Coat-hanger test

Mice were placed to hang at the center of the horizontal bar (diameter, 3 mm; length, 40 cm) situated at a height of 50 cm from a mat-covered floor. The prehensile reflex was evaluated by scoring the behavior on the bar as it follows: (0) fell off the hanger within 10 s; (1) hang for 10 s with two forepaws on the hanger; (2) attempted to climb the hanger; (3) hang onto bar by two forepaws and at least one hindpaw on the hanger; (4) all four paws and tail wrapped around the hanger; (5) active escape to the end of the hanger. The mice were observed during a single 3-trial session with a 1 min cut-off period and a 30-min intertrial interval.

Open field test

Mice were tested in the open field to assess locomotor activity, exploratory and anxiety-related behavior as previously described[9]. Mice were placed in the center of a square arena (62 cm × 62 cm) at the start of the test. Locomotor activity was monitored for 10 min with a computerized tracking system (Anilab, Ningbo, China). Total distance, speed, and time spent in the center square were recorded.

Filipin staining

HeLa cells or 10-μm brain cryosections were fixed with 4 % PFA for 15 min at room temperature (RT). After postfixing with 4 % PFA and rinsing with PBS, cells or cryosections were incubated with 1.5 mg/ml glycine in PBS for 10 min. Then, cells or cryosections were stained with 300 μg/ml Filipin (Sigma-Aldrich, SAE0088) in the dark for 2 h at RT. After three washes with PBS, cells or cryosections were imaged directly.

Off-target detection

We used http://crispor.tefor.net/ to identify five potential off-target sites for the sgRNA in the genome. We extracted genomic DNA from the tails of *Clcn6*$^{E200A/+}$, *Clcn6*$^{-/-}$ mice, and PCR-amplified five pre-selected potential off-target sites from three *Clcn6*$^{E200A/+}$ mice and four *Clcn6*$^{-/-}$ mice. We validated off-target effects by the sequencing of the PCR products using Sanger procedures.

Survival analysis

The Kaplan-Meier method was used to determine the survival rates of the mice ($n \geq 12$ per genotype). When the mice were unable to access food and water, which was considered the endpoint, the mice were euthanized for animal welfare reasons. For each mouse, the age (in days) at which they were killed was recorded.

Hind limb extension test

All mice underwent the hind limb extension test at the ages of 2 months as reported previously[10]. Briefly, each mouse was suspended by the tail at a height of approximately 50 cm to provoke a clasping phenotype. The hind limb spreading reflex and clasping behavior were assessed.

Tissue collection and preparation

For histology, immunofluorescence and immunohistochemistry analysis, mice were deeply anesthetized by intraperitoneal injection using 0.1 g/ml ethyl carbamate (Solarbio, 1994-9-7) and perfused transcardially with phosphate buffer solution (PBS) followed by 4 % paraformaldehyde (PFA, w/v) in PBS. Eyes or brains were carefully removed and postfixed overnight in 4 % PFA at 4 °C, then dehydrated, embedded in OCT compound or paraffin. Samples were subsequently sectioned with 10-μm Cryostat sagittal sections or 3-μm paraffin sagittal sections. For Western blot, qRT-PCR, and enzyme activity analysis, mice were anaesthetized, perfused with ice-cold PBS, brain or liver tissues were collected and kept at -80 °C for prior to analysis or used directly for analytical experiments.

Determination of brain weights

Brain weights were determined for P30 and 4-month-old WT, *Clcn6*$^{E200A/+}$ and *Clcn6*$^{-/-}$ mice. Mice were deeply anesthetized with isoflurane. In order to assess whether lower brain weight was associated with lower body weight. Body weights were obtained prior to killing these mice, then brains were quickly dissected and weighed.

Cortical thickness measurement

Regional volume measurements of cortical thickness were obtained using CaseViewer software. Regions of interest (ROIs) of regional volume were obtained using the 5-μm-thick Nissl-stained sections. The thickness is defined as the length of streamlines crossing cortical layers in perpendicular. We measured the maximum length of the primary motor (M1), S1 cortex hindlimb region (S1HL), secondary visual cortex mediolateral area (V2ML), and secondary visual cortex mediomedial area (V2MM).

RNA extraction and qRT-PCR

Total RNA from brain of 4-to-5-month-old WT (n = 8), *Clcn6*$^{E200A/+}$ (n = 4), and *Clcn6*$^{-/-}$ (n = 4) mice were isolated using TRIzol® reagent according to the manufacturer's protocol. The RNA samples were reverse transcribed and converted to cDNA using the Hiscript II Q RT SuperMix cDNA Synthesis kit (Vazyme). Expression of mRNA was

quantified using a SYBR Green PCR Master Mix (Vazyme). Primer sequences are listed in Supplemental Table 4. PCR amplification was performed under the following conditions: 95 °C for 5 min, followed by 40 cycles of: 95 °C for 10 s and 60 °C for 30 s, then post holding stage: 95 °C for 15 s, 60 °C for 1 min and 95 °C for 1 s. Gene expression data was analyzed using the $2^{-\Delta\Delta Ct}$ method with *Gapdh* as control.

Western blot

For Western blot analysis, HeLa cells were collected two days after transfection and lysed in cold RIPA buffer (Beyotime Biotechnology) with protease inhibitors (Bimake). Mouse tissues were homogenized in the same lysis buffer with protease and phosphatase inhibitors (Bimake), followed by sonication and centrifugation. Equal amounts of protein were separated by SDS-PAGE and transferred onto polyvinylidene difluoride membranes. Membranes were probed with primary antibodies followed by incubation with horseradish peroxidase-conjugated secondary antibodies. After washing, blots were analyzed with enhanced chemoluminescence.

Histological and histochemical analyses

Hematoxylin and eosin (H&E), Nissl, Luxol Fast Blue, and Periodic Acid Schiff (PAS) staining were performed on dewaxed and rehydrated 5-µm paraffin sections according to standard procedures.

For immunohistochemistry, 5-µm sagittal sections from paraffin-embedded brains were dewaxed, subjected to antigen retrieval in citrate buffer with heat, and incubated for 5 min with 3 % H_2O_2 in PBS to reduce endogenous peroxidase activity. After 1 h blocking in 3 % bovine serum albumin (BSA), 0.3 % Triton-X in PBS, brain sections were then incubated with specific primary antibodies overnight at 4 °C. After three washes with PBS, samples were incubated with secondary antibody for 1 h at RT. Samples were then stained for DAPI (1:1000), embedded with Fluoromount-G mounting medium. For immunofluorescence, HeLa cells transfected with the respective ClC-6 construct in glass-bottom dishes were washed with PBS, followed by fixation with 4 % PFA. Immunostaining was conducted as described previously[4]. 10-µm brain cryosections were fixed with 4 % PFA for 15 min at RT, permeabilized in 0.3 % PBST (0.3 % Triton X-100 in PBS) for 20 min, and blocked for 30 min in 3 % BSA in 0.2 % PBST before overnight incubation at 4 °C with primary antibodies, followed by secondary antibodies conjugated with Alexa Fluor (Thermo Fisher Scientific, Alexa Fluor Goat anti-rat 488, Goat anti-rabbit 594) in 3 % BSA for 1 h at RT. Nuclei were stained with DAPI for 5 min. Finally, sections were mounted onto slides and fluorescent images were acquired with a laser scanning confocal microscope (LSM 900, Carl Zeiss, Oberkochen, Germany) using a 63x/1.4 NA oil immersion objective lens. For autofluorescence, unstained 5-µm sagittal sections from paraffin-embedded brains were examined as described previously[4]. Brain sections were

coverslipped with Fluoromount-G, and imaged directly. Autofluorescence was detected using a TRITC filter set (AHF Analysetechnik; Ex 543/22, DC 562, Em 593/40) on a DMi8 microscope (Leica Microsystems).

For transmission electron microsocopic analyses, thin tissue slices (1×1×1mm) of perfused brains were fixed in 2.5 % glutaraldehyde and 1 % osmium tetroxide for 24 h at 4 °C, followed by three washings in Millonig's phosphate buffer at RT. After dehydration through a graded series of ethanol, samples were infiltrated in a mixture of epon substitute and araldite for 4 h, then baked at 60 °C for 48 h. Ultra-thin 60-80-nm sections were cut, stained with lead citrate and uranyl acetate, and examined with a Hitachi (Tokyo, Japan) H7000 transmission electron microscope.

LysoTracker Deep Red staining

10^5 HeLa cells were plated on 35-mm glass-bottom dishes (MatTek). On the next day, cells were transfected with GFP-tagged ClC-6 plasmids. Cells were incubated 30 min with prewarmed 50 nM LysoTracker Deep Red (Thermo Fisher) at 37 °C. Cells were then washed 2 times with PBS and imaged in live imaging buffer containing 135 mM NaCl, 5 mM KCl, 1mM $CaCl_2$, 1 mM $MgCl_2$, 10 mM glucose, 25 mM HEPES (pH 7.4). Images were acquired with a DMi8 microscope (Leica Microsystems) with 647 nm excitation and detection at 668 nm.

Cathepsin D activity measurement

The proteolytic activity of Cathepsin D (CTSD) was determined using a Fluorometric CTSD Activity Assay Kit (Abcam). After washing with ice-cold PBS, cerebral cortical tissues were homogenized in 1 mL of CD Cell Lysis buffer on ice. Tissue homogenates were centrifuged at 13,500 g for 5 min at 4 °C to remove any insoluble material. The protein concentration was determined by the BCA method. Then, 50 μg of protein were mixed with 50 μL reaction buffer and 2 μL substrate, and incubated in dark for 1 h at 37 °C. The activity was measured by using a fluorescence microplate reader at an excitation wavelength of 328 nm and an emission wavelength of 460 nm. The relative fluorescence units (RFU) were normalized with total protein amount of each sample.

Results

Clinical feature of the proband

A 10-year-old girl initially presented with developmental delay, she rolled at 7 months, sat up without support at 8 months, walked at 2 years. She had unremarkable perinatal, neonatal and family history. At the age of 3 years, she experienced her first seizure. The girl had variable type of seizures including focal, myoclonic, atypical absence and generalized tonic-clonic seizures. She was treated with sodium valproate, topiramate, zonisamide, clonazepam, lamotrigine, oxcarbazepine, and levetiracetam. She responded with a significant seizure reduction to the combined therapy of topiramate, oxcarbazepine, and levetiracetam after several unsuccessful anti-seizure drug trials. Soon after, she lost expressive language. At 4 years, she developed progressive ataxia, and some stereotypic hand movements. In the following years, she exhibited a progressive neurological decline and dystonic posturing. By the age of 6 years and 7 months, she lost her walking ability, and became wheelchair-dependent. Currently, she has few seizures and limited hand function, is unable to stand independently, but she can change from a supine to a sitting position. She has feeding difficulties. No facial dysmorphism was noticed. Her head circumference was 45.5 cm at 3 years 4 months (< 3rd centile). Her deep tendon reflexes were essentially normal. When last reviewed at 10 years of age, her weight was 20 kg (< 3rd centile), height approximately 120 cm (< 3rd centile), and head circumference was 48.5 cm (< 3rd centile). The fundus examination was unremarkable. Her karyotype was 46, XX. Whole-exome sequencing revealed that she was heterozygous for a *CLCN6* c.599A>C, p.E200A variant, which was validated *de novo* by Sanger sequencing.

Supplemental figures

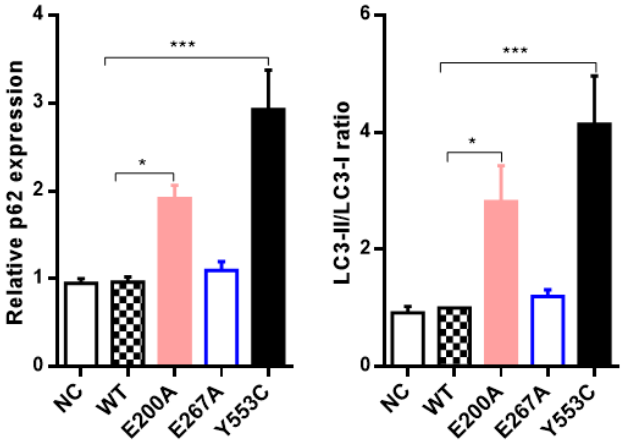

Figure S1 Western blot analysis of autophagy-related proteins in transfected HeLa cells. Quantification of Western blot analysis as in Figure 2A showed that the protein levels of SQSTM1/p62 and the LC3-II /LC3-I ratio were increased in ClC-6 p.E200A or p.Y533C-expressing cells, but not changed in ClC-6 p.E267A-expressing cells. β-actin was used for normalization. Values are expressed as mean ± SEM. One-way ANOVA or nonparametric with Tukey's multiple-comparison test. *p < 0.05, ***p < 0.001.

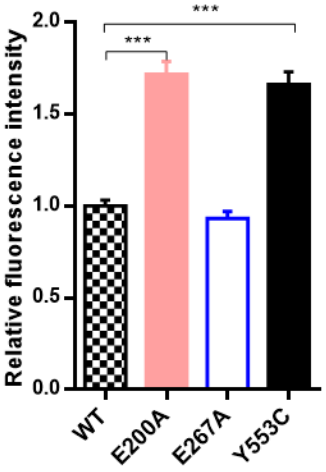

Figure S2 Filipin staining in transfected HeLa cells. Quantification of Filipin staining as in Figure 2D showed that cells expressing ClC-6^{E200A} or ClC-6^{Y553C} mutants had more Filipin staining than cells expressing WT ClC-6 or ClC-6^{E267A} mutant. Values are expressed as mean ± SEM. One-way ANOVA with Tukey's multiple-comparison test. ***p < 0.001.

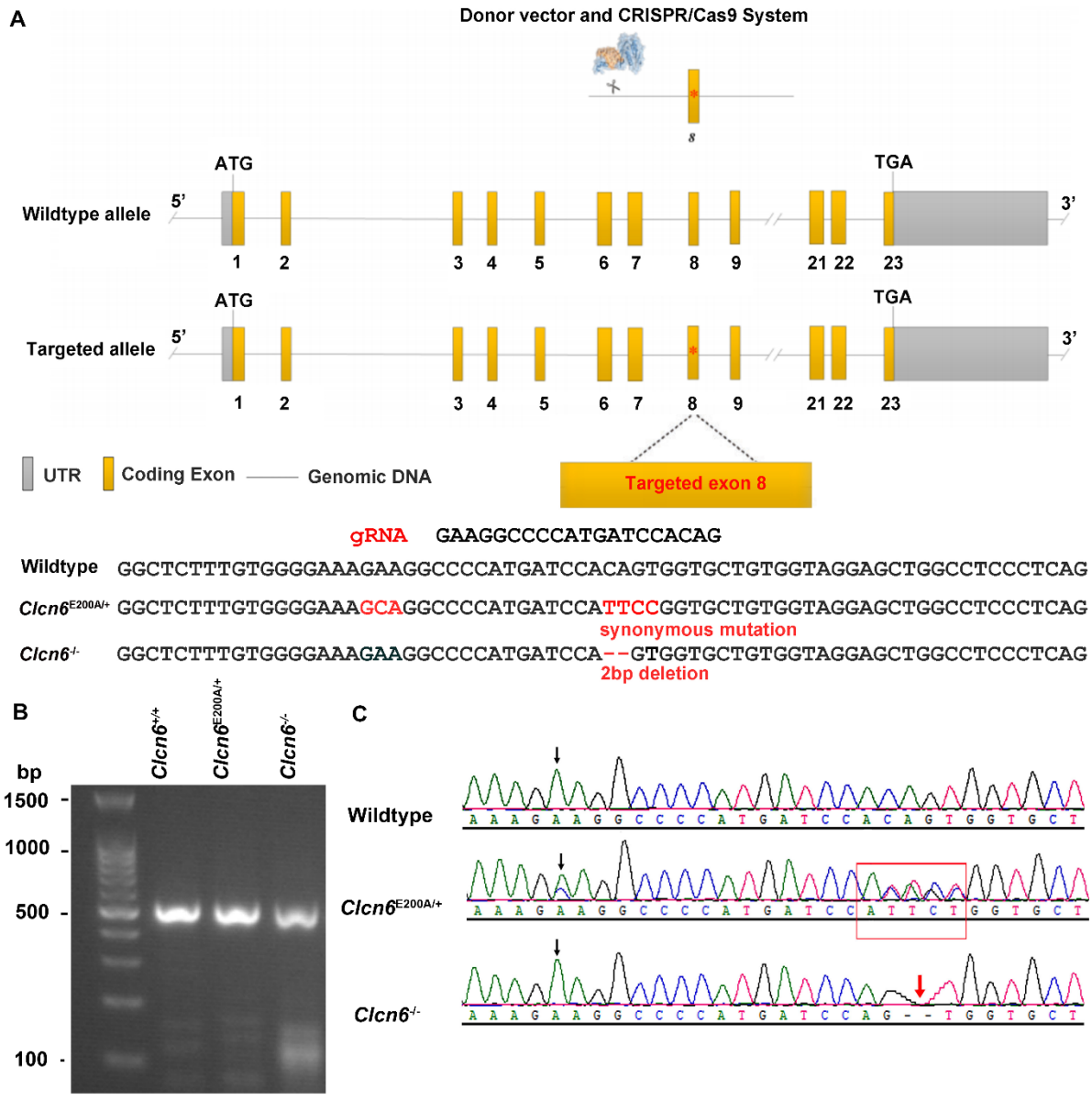

Figure S3 Generation and validation of *Clcn6*$^{E200A/+}$ and *Clcn6*$^{-/-}$ mice. (A) Schematic depiction of gene targeting strategy. Exon 8 was modified by inserting the c.599 A>C, p.E200A mutation and additionally two synonymous mutations to avoid repeat excision. (B) Representative agarose gel PCR genotyping of tail biopsy DNAs from mice of all three genotypes. (C) DNA sequence results of representative wildtype (WT), heterozygous *Clcn6*$^{E200A/+}$ and homozygous *Clcn6*$^{-/-}$ mice.

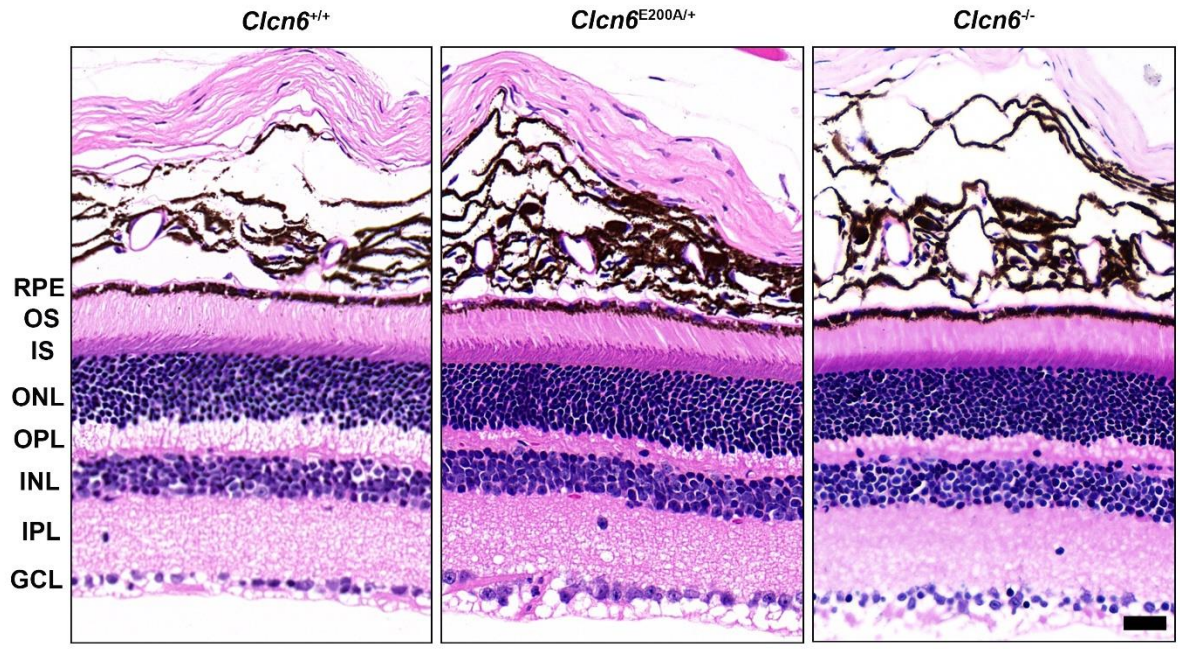

Figure S4 H&E retina staining. Paraffin sections of the retina at 5 months of age revealed no retinal degeneration in both *Clcn6*$^{E200A/+}$ and *Clcn6*$^{-/-}$ mice after H&E staining. Abbreviations are as follows: RPE retinal pigment epithelium; OS photoreceptor outer segments; IS photoreceptor inner segments; ONL outer nuclear layer; OPL outer plexiform layer; INL inner nuclear layer; IPL inner plexiform layer; GCL ganglion cell layer. n ≥ 3 per genotype. Scale bar: 20 μm.

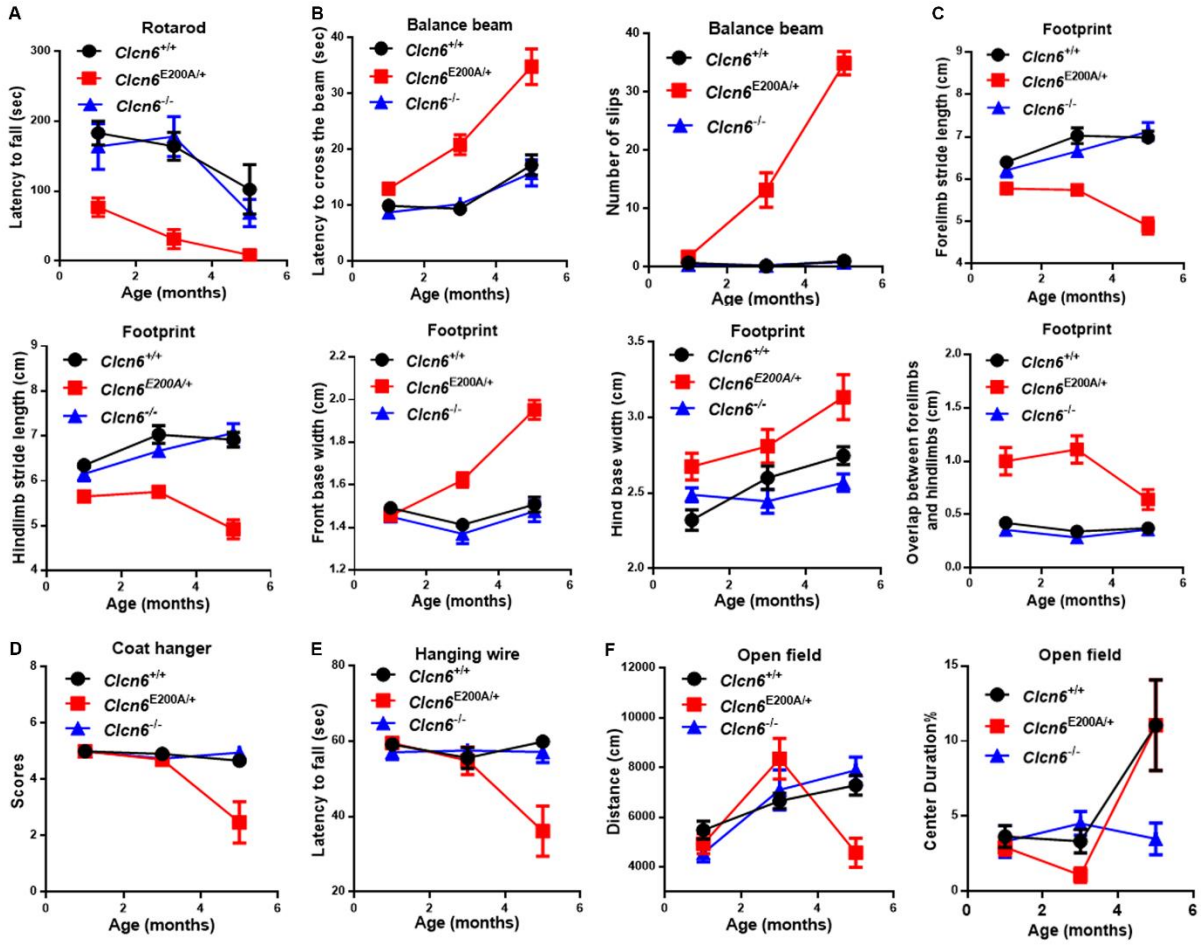

Figure S5 Behavioral phenotypes of *Clcn6*$^{E200A/+}$ and *Clcn6*$^{-/-}$. (A) In the rotarod test, *Clcn6*$^{E200A/+}$ mice showed a shorter latency to fall off the rod at 1, 3, 5 months. (B) In the balance beam test, *Clcn6*$^{E200A/+}$ mice showed a longer latency to cross the beam at 1, 3, 5 months, and a higher number of foot slips at 3, 5 months. (C) In the footprint analysis, *Clcn6*$^{E200A/+}$ had a significantly shorter forelimb and hindlimb stride length, wider hindlimb base length and overlap length between forelimb and hindlimb starting at 1, 3, 5 months, and a wider front base width at 3,5 months, compared to WT mice. (D) In the coat hanger test, *Clcn6*$^{E200A/+}$ mice scored lower than WT controls at 5 months. (E) In the hanging wire test, there was a dramatic reduction in the ability of *Clcn6*$^{E200A/+}$ mice to hang onto the wire at 5 months. (F) In the open field test, *Clcn6*$^{E200A/+}$ mice traveled a longer total distance at 3 months, but less spontaneously at 5 months. *Clcn6*$^{E200A/+}$ mice spent less time in the center field at 3 months, and *Clcn6*$^{-/-}$ mice spent less time in the center field at 5 months. Data were analyzed by one-way ANOVA with Tukey's multiple-comparison test for $n \geq 7$ per genotype and presented as mean ± SEM.

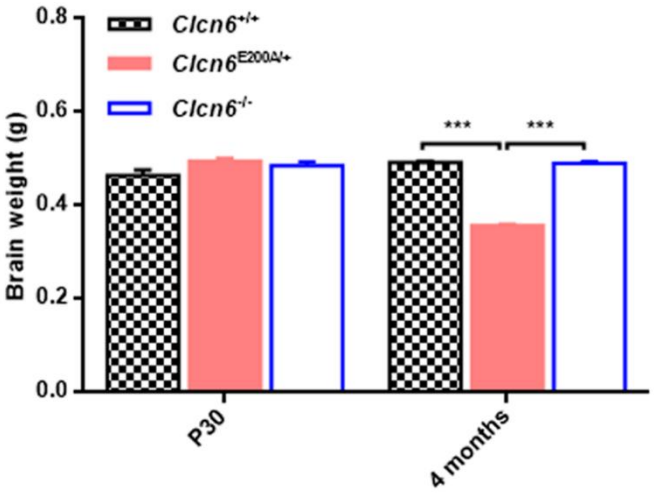

Figure S6 Brain weights of *Clcn6*$^{E200A/+}$, *Clcn6*$^{-/-}$ and WT mice. Brain mass was reduced in *Clcn6*$^{E200A/+}$ mice at 4 months when compared to age matched WT controls. Brain weights of *Clcn6*$^{-/-}$ mice are used for comparison. Data were analyzed by one-way ANOVA with Tukey's multiple-comparison test for n ≥ 3 per genotype and presented as mean ± SEM, ***p < 0.001.

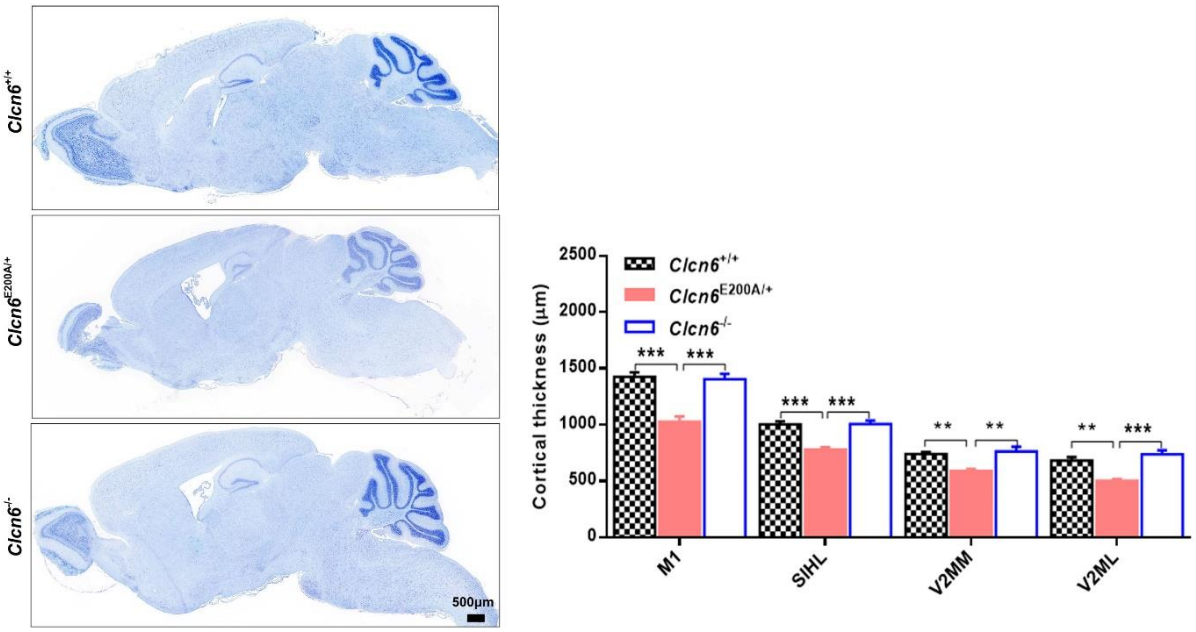

Figure S7 Cortex thickness of *Clcn6*$^{E200A/+}$, and *Clcn6*$^{-/-}$ mice at 5 months. Cortex thickness decreased in primary motor (M1), S1 cortex hindlimb region (S1HL), secondary visual cortex mediolateral area (V2ML), and secondary visual cortex mediomedial area (V2MM) in 5-month-old *Clcn6*$^{E200A/+}$ mice compared with age-matched WT or littermates, but not in 5-month-old *Clcn6*$^{-/-}$mice. Data were analyzed by one-way ANOVA with Tukey's multiple-comparison test for n ≥ 3 per genotype and presented as mean ± SEM, **p < 0.01, ***p < 0.001. Scale bar: 500 μm.

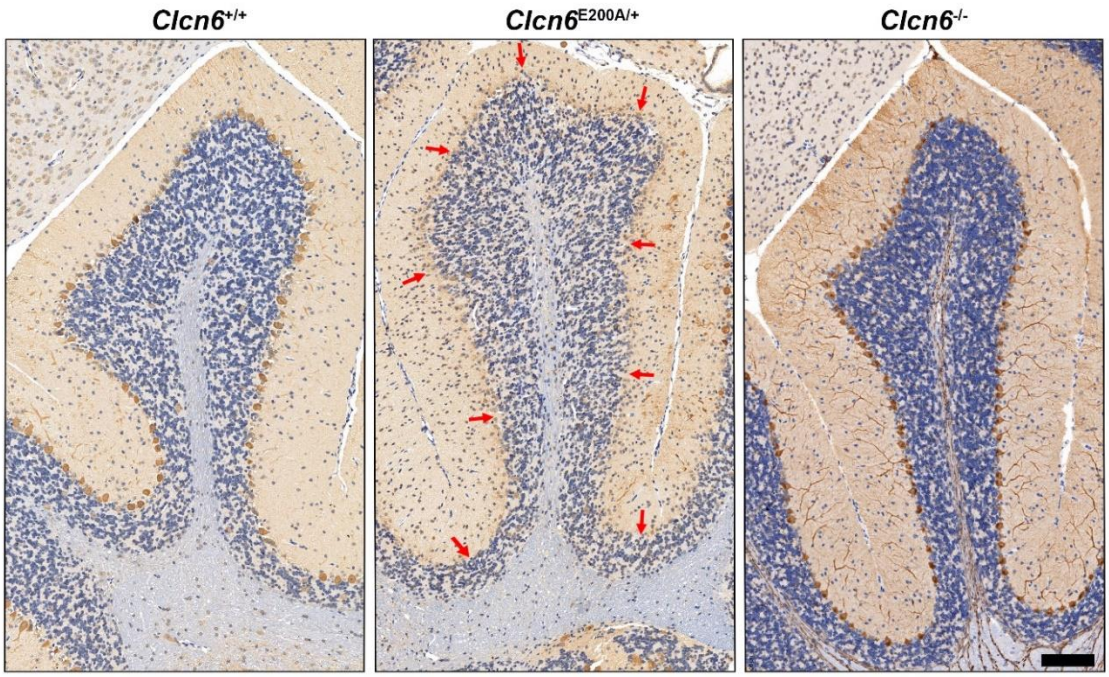

Figure S8 Loss of Purkinje cells. Immunohistochemical staining for the Purkinje cell marker calbindin revealed a prominent loss of Purkinje cells in 5-month-old *Clcn6*$^{E200A/+}$ mice, but not in *Clcn6*$^{-/-}$ mice. Shown are the lobule III of the cerebellum from 5-month-old *Clcn6*$^{+/+}$, *Clcn6*$^{E200A/+}$ and *Clcn6*$^{-/-}$ mice (n = 4 per genotype). Scale bar: 100 µm.

Figure S9 Nissl staining. A representative Nissl-stained sagittal brain section from a 20-month-old *Clcn6*$^{-/-}$ mouse. N = 4. Scale bar: 500 µm.

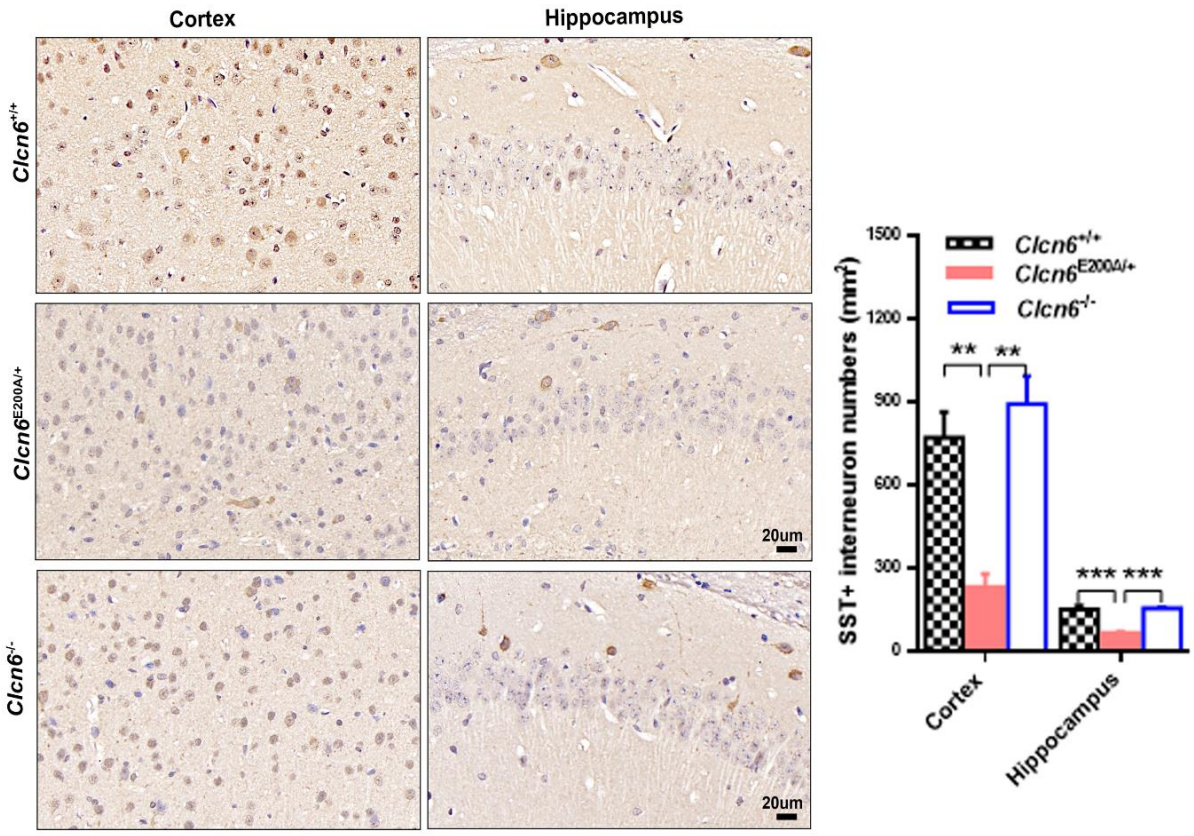

Figure S10 Immunohistochemical staining for somatostatin (SST). The loss of SST+ interneurons was evident in the cortex (representative images of the medial parietal association cortex) and hippocampus of *Clcn6*$^{E200A/+}$ mice at 5 months compared to age-matched WT or littermates. Data were analyzed by one-way ANOVA with Tukey's multiple-comparison test for $n \geq 3$ per genotype and presented as mean ± SEM, $^{**}p < 0.01$, $^{***}p < 0.001$. Scale bar: 20 μm.

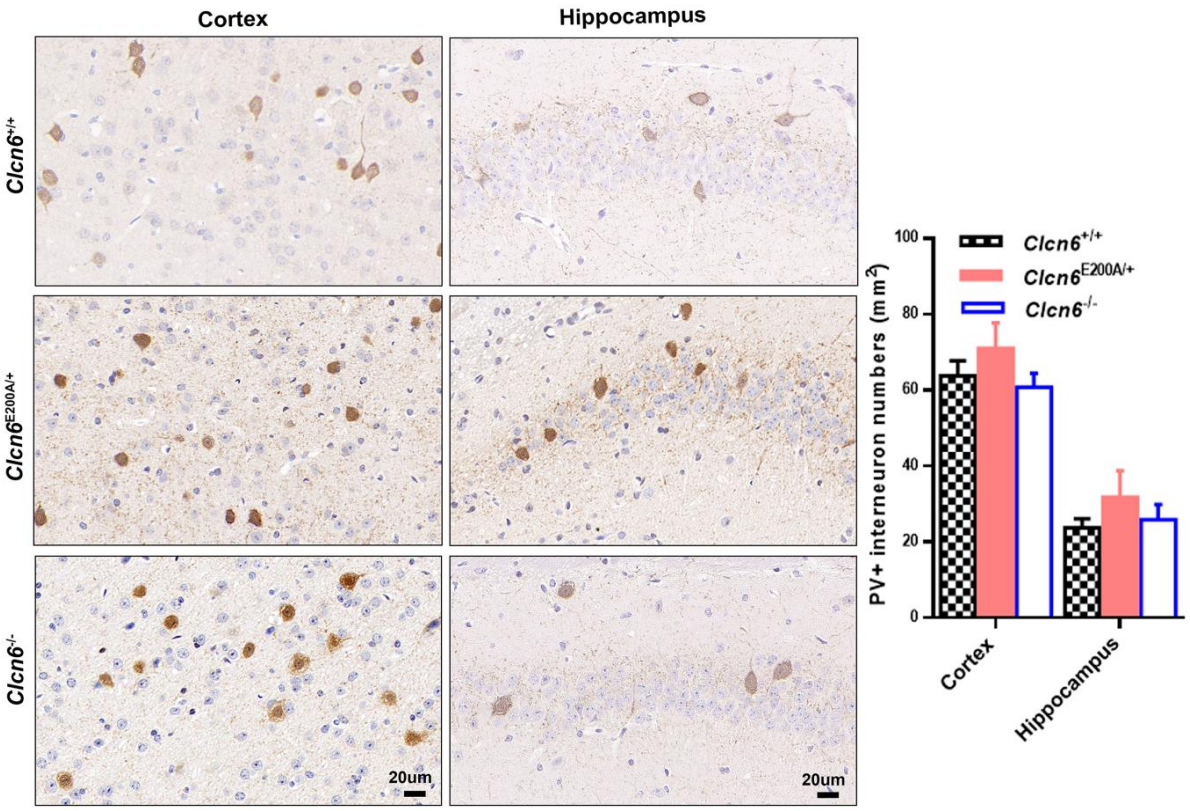

Figure S11 Immunohistochemical staining for parvalbumin (PV). There was no change in the number of PV+ interneurons in the cortex (representative images of the primary motor cortex) or hippocampus of *Clcn6*$^{E200A/+}$ mice at 5 months compared to age-matched WT or littermates. Data were analyzed by one-way ANOVA with Tukey's multiple-comparison test for $n \geq 3$ per genotype and presented as mean ± SEM. Scale bar: 20 μm.

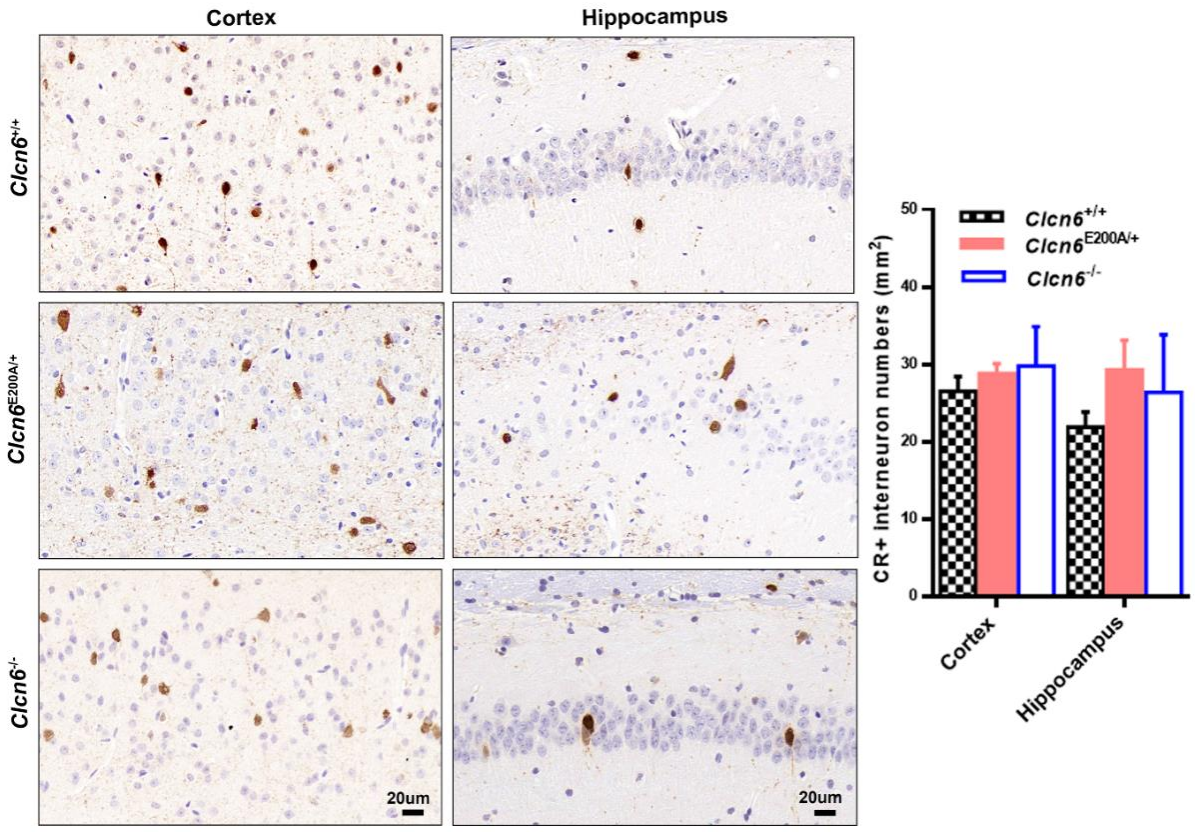

Figure S12 Immunohistochemical staining for calretinin (CR). There was no change in the number of CR+ interneurons in the cortex (representative images of the medial parietal association cortex) or hippocampus of *Clcn6*$^{E200A/+}$ mice at 5 months compared to age-matched WT or littermates. Data were analyzed by one-way ANOVA with Tukey's multiple-comparison test for n ≥ 3 per genotype and presented as mean ± SEM. Scale bar: 20 µm.

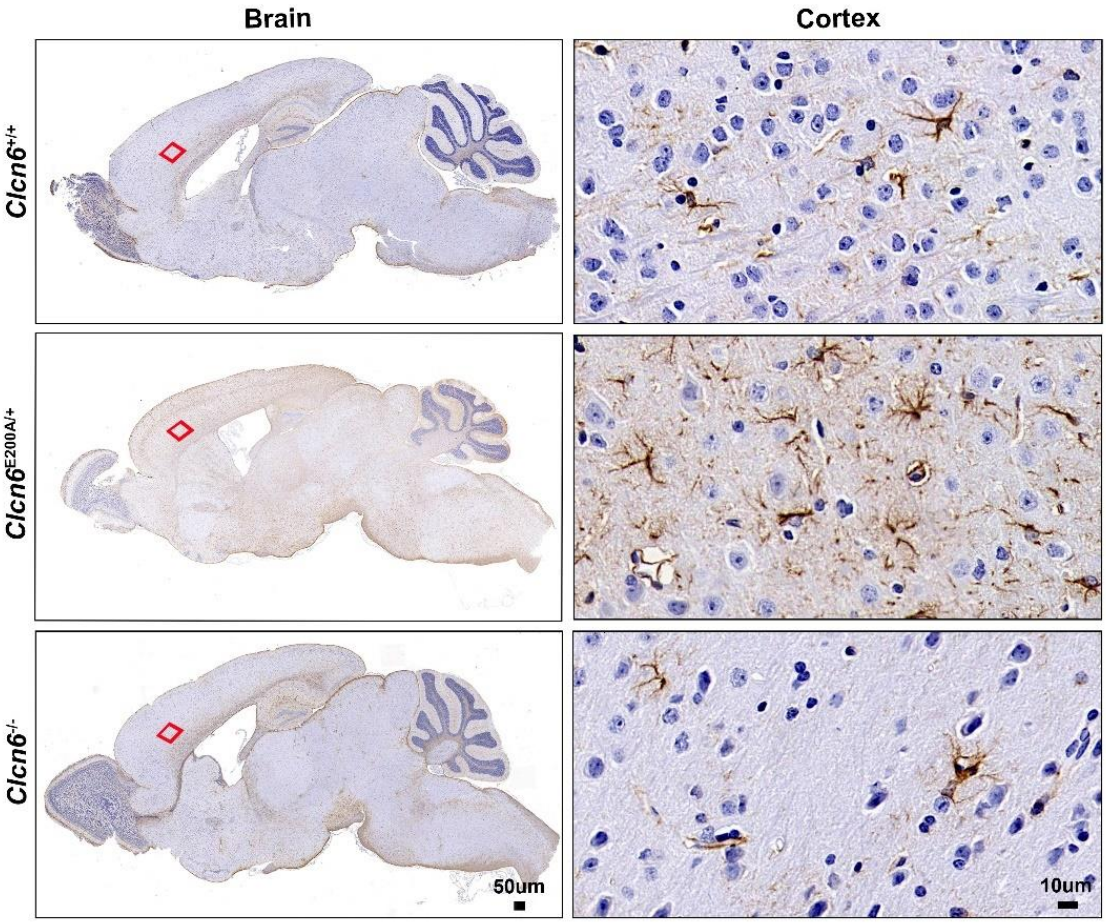

Figure S13 Immunohistochemical staining for the astrocyte marker glial fibrillary acidic protein (GFAP) in 4-5 months old mice. Widespread astrocytosis was evident in the brain of *Clcn6*$^{E200A/+}$ mice at 4-5 months compared to age-matched WT or littermates, but not in 4-to-5-month-old *Clcn6*$^{-/-}$ mice. Representative images of the secondary motor cortex are shown in the enlargement. n ≥ 3 per genotype. Scale bars: 50 µm and 10 µm, respectively.

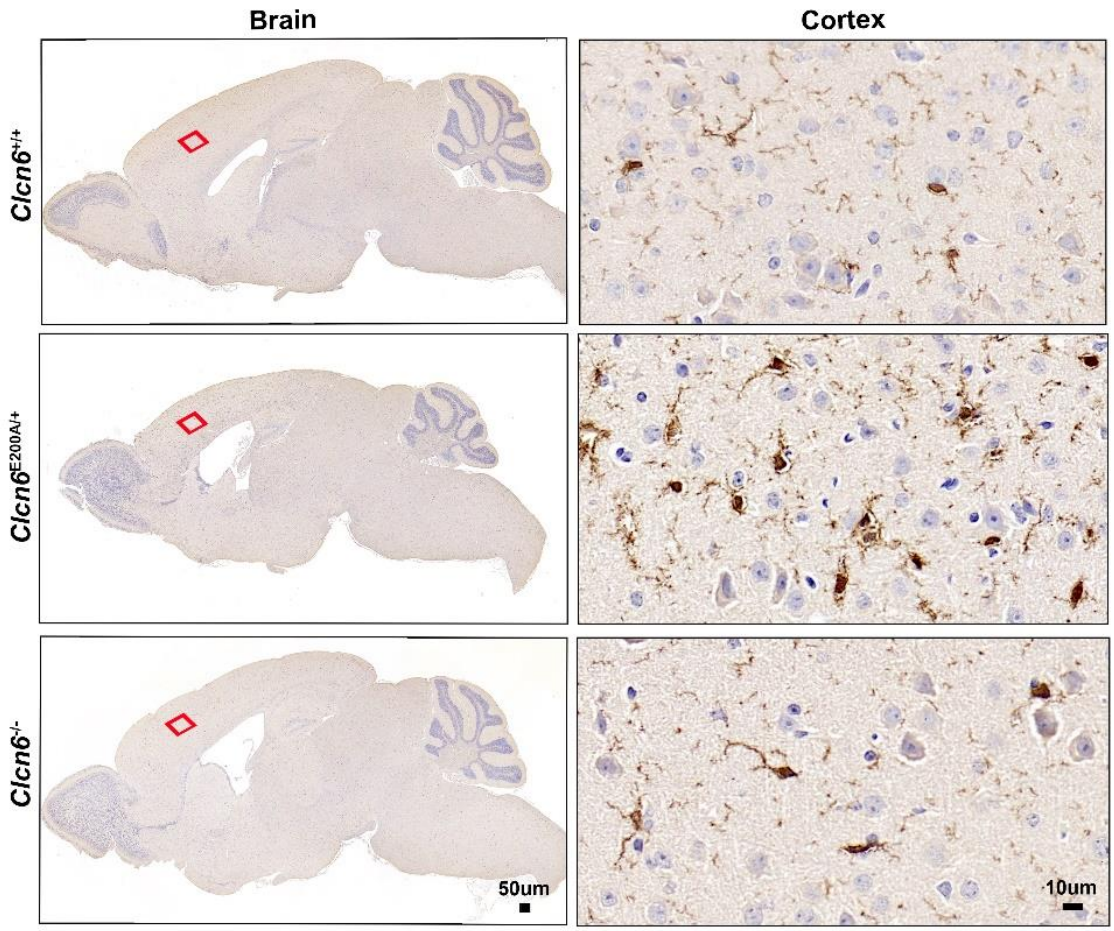

Figure S14 Immunohistochemical staining for the microglial marker IBA-1 in 4-5 months old mice. Widespread microgliosis in the brain of *Clcn6*$^{E200A/+}$ mice at 4-5 months compared to age-matched WT or littermates, but not in 4-to-5-month-old *Clcn6*$^{-/-}$ mice. Representative images of the secondary motor cortex are shown in the enlargement. n ≥ 3 per genotype. Scale bars: 50 µm and 10 µm, respectively.

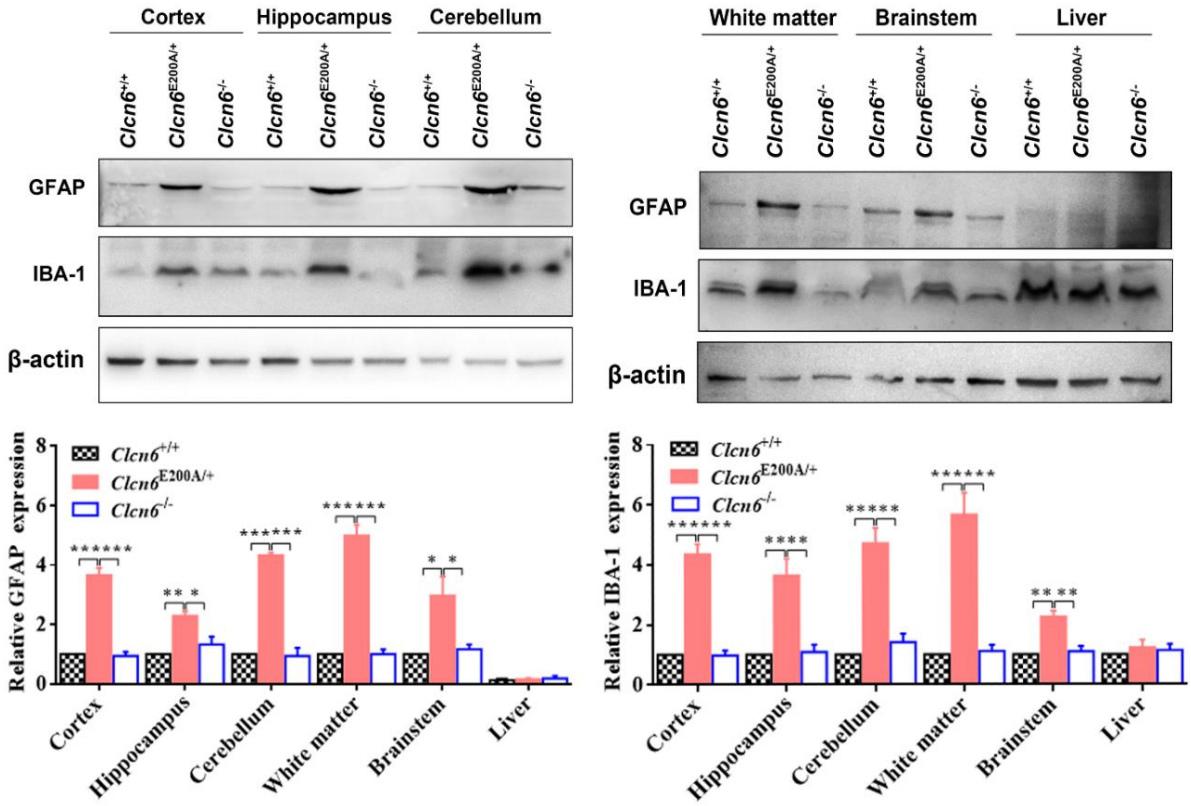

Figure S15 Protein levels of GFAP and IBA-1 in 5-month-old mice. Quantification of Western blot analysis showed a strong increase of GFAP and IBA-1 in the cortex, hippocampus, cerebellum, white matter and brainstem, but not in the liver of 5-month-old *Clcn6*$^{E200A/+}$, but not *Clcn6*$^{-/-}$ mice compared to age-matched WT mice or littermates. Data were analyzed by one-way ANOVA or nonparametric with Tukey's multiple-comparison test for $n \geq 3$ per genotype and presented as mean ± SEM, *$p < 0.05$, **$p < 0.01$, ***$p < 0.001$.

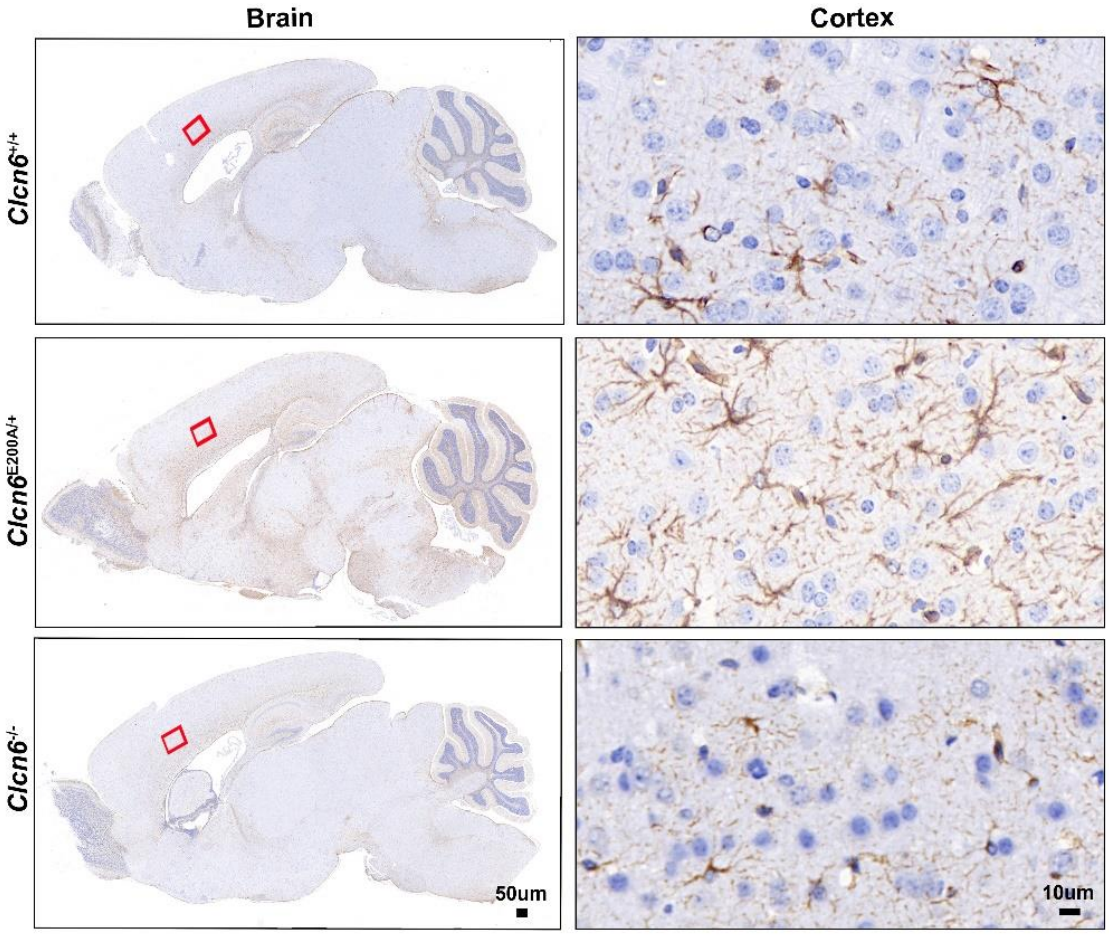

Figure S16 Immunohistochemical staining for GFAP in postnatal day 30 (P30) mice. Astrogliosis was observed in many brain regions of *Clcn6*$^{E200A/+}$ mice at P30 compared to age-matched WT mice, but not in P30 *Clcn6*$^{-/-}$ mice. Representative images of the secondary motor cortex are shown in the enlargement. n ≥ 3 per genotype. Scale bars: 50 μm and 10 μm, respectively.

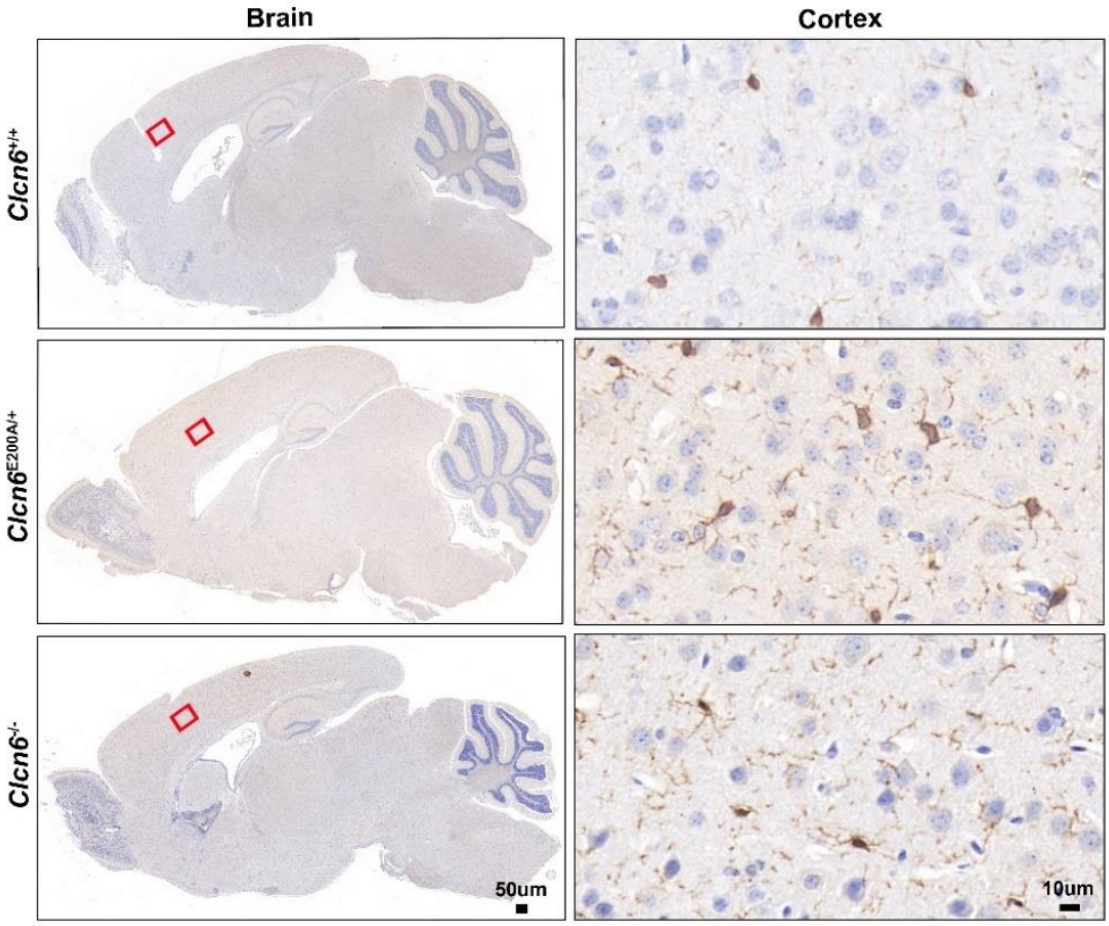

Figure S17 Immunohistochemical staining for IBA-1 in P30 mice. Microgliosis was observed in many brain regions of *Clcn6*$^{E200A/+}$ mice at P30 compared to age-matched WT mice, but not in P30 *Clcn6*$^{-/-}$ mice. Representative images of the secondary motor cortex are shown in the enlargement. n ≥ 3 per genotype. Scale bars: 50 μm and 10 μm, respectively.

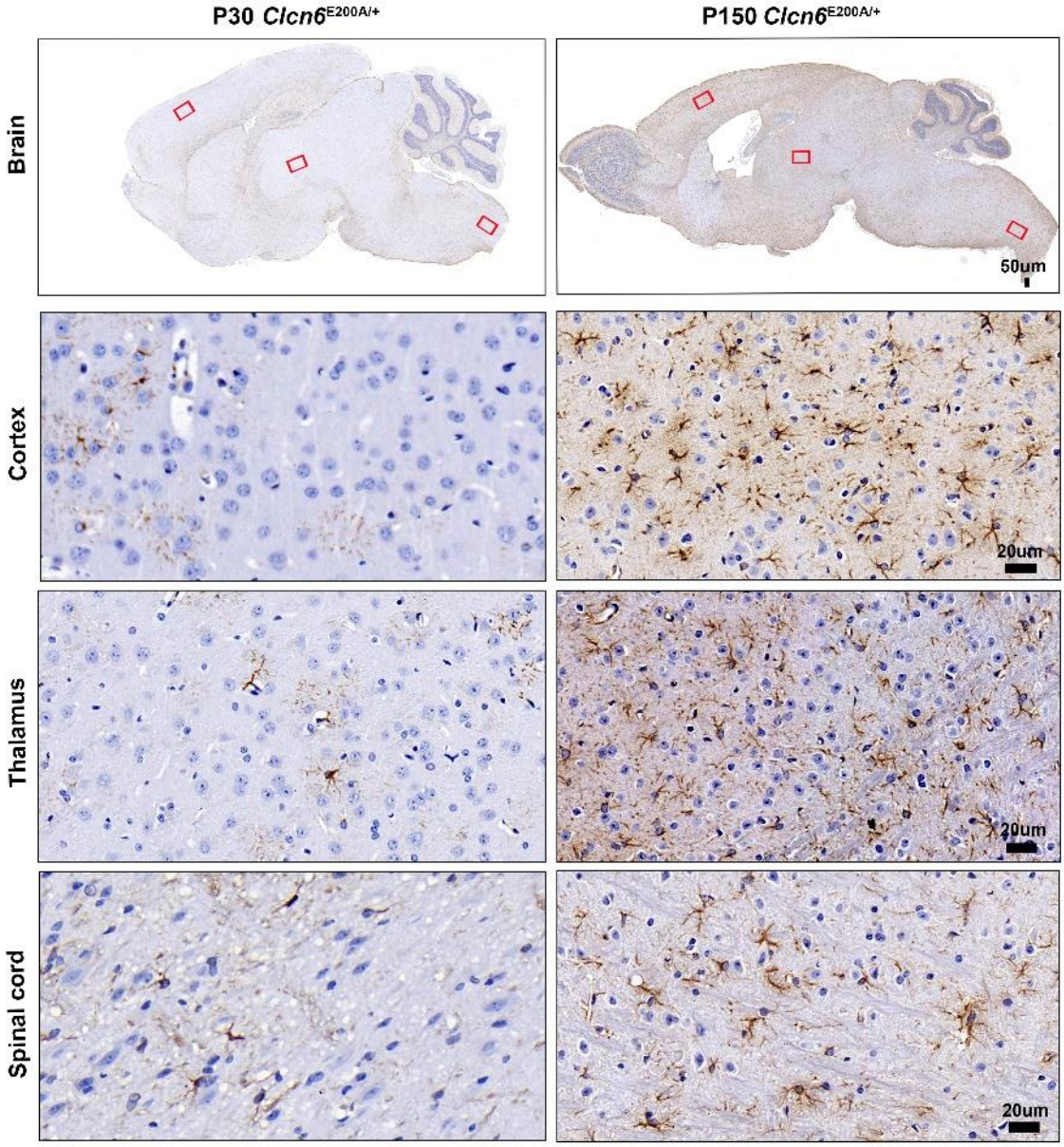

Figure S18 Immunohistochemical staining for GFAP in P30 and P150 *Clcn6*$^{E200A/+}$ mice. Activation of astrocytes in the brain of *Clcn6*$^{E200A/+}$ mice was detectable at P30 and progressed in density and intensity at P150. Representative images of the secondary motor cortex (upper left red box in the overview), thalamus (middle red box), and spinal cord (lower right red box) are shown in the enlargements. $n \geq 3$ per genotype. Scale bars: 50 µm.

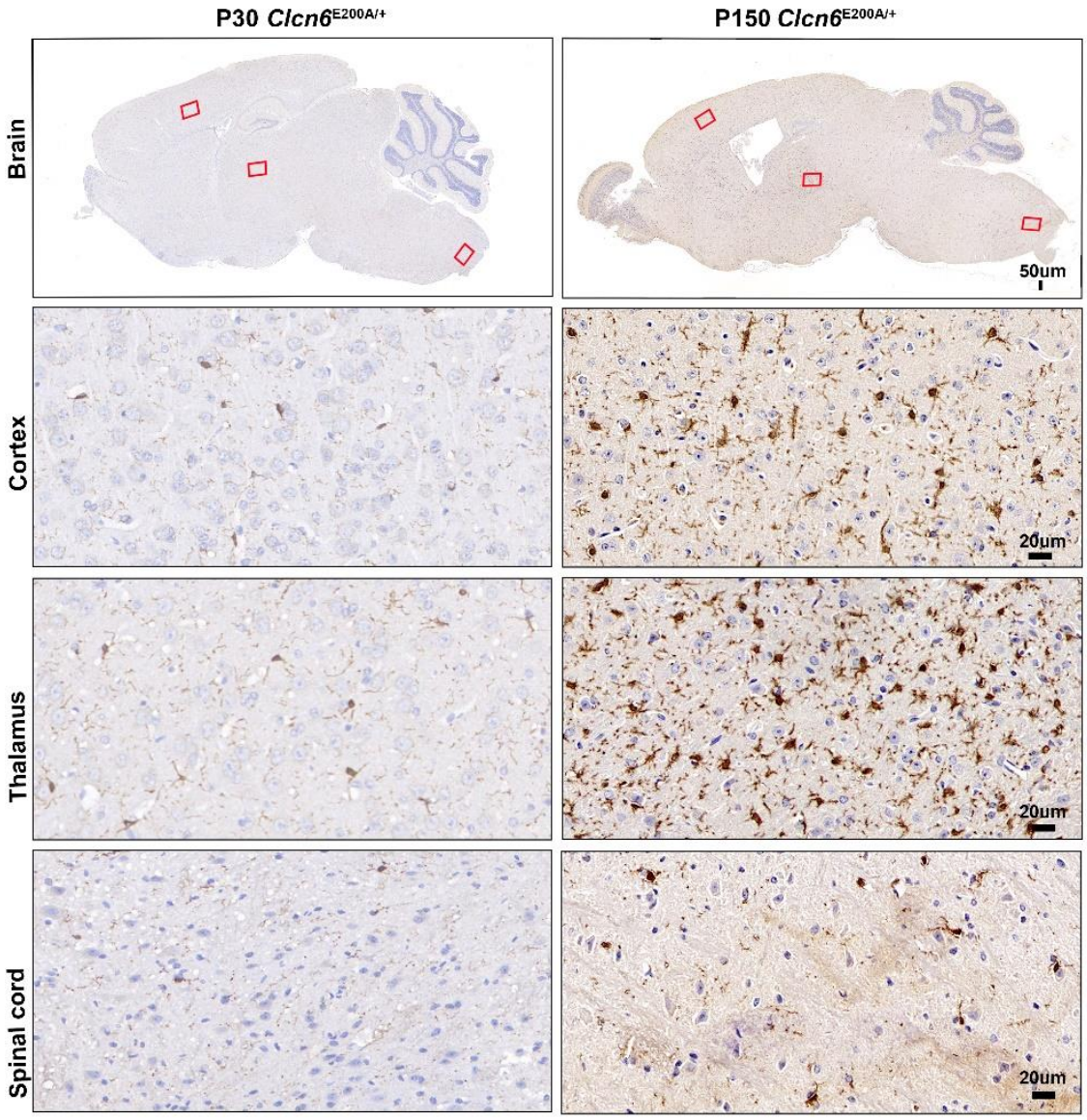

Figure S19 Immunohistochemical staining for IBA-1 in P30 and P150 *Clcn6*$^{E200A/+}$ mice. Activation of microglia in the brain of *Clcn6*$^{E200A/+}$ mice was detectable at P30 and progressed in density and intensity at P150. Representative images of the secondary motor cortex (upper left red box in the overview), thalamus (middle red box), and spinal cord (lower right red box) are shown in the enlargements. n ≥ 3 per genotype. Scale bars: 50 µm.

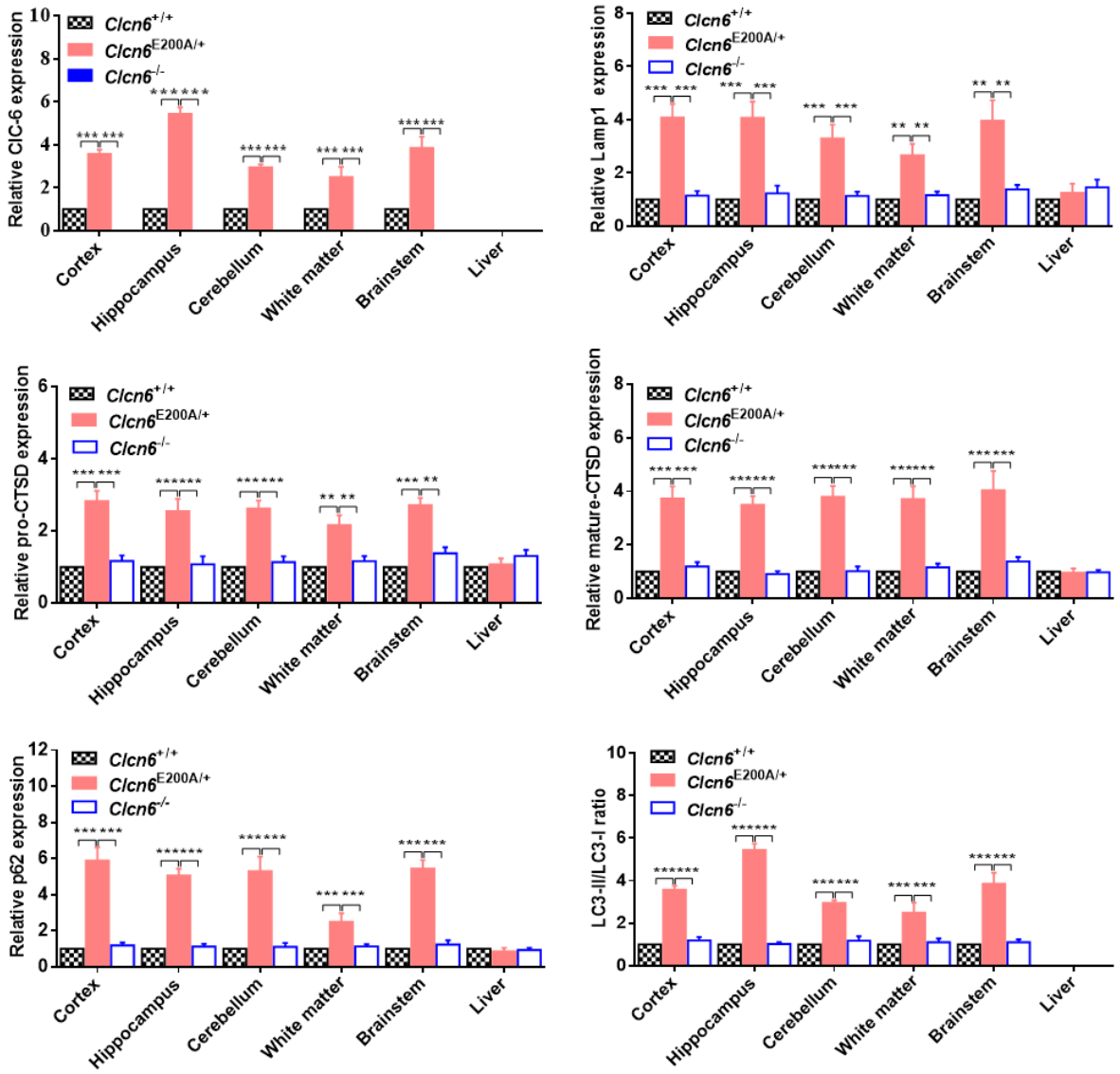

Figure S20 Lysosomal and autophagic protein levels in P120 mice. Quantification of Western blot analysis (as in Figure 7A) showed a strong increase of ClC-6, Lamp1, SQSTM1/p62, pro-cathepsin D (pro-CTSD), mature-CTSD and LC3-II/ LC3-I in the cortex, hippocampus, cerebellum, white matter and brainstem, but not in the liver from 5-month-old *Clcn6*$^{E200A/+}$ mice compared to WT or littermates. *Clcn6*$^{-/-}$ mice are used for comparison. All data were analyzed by one-way ANOVA or nonparametric with Tukey's multiple-comparison test for n ≥ 4 per genotype and presented as mean ± SEM, **p < 0.01, ***p < 0.001.

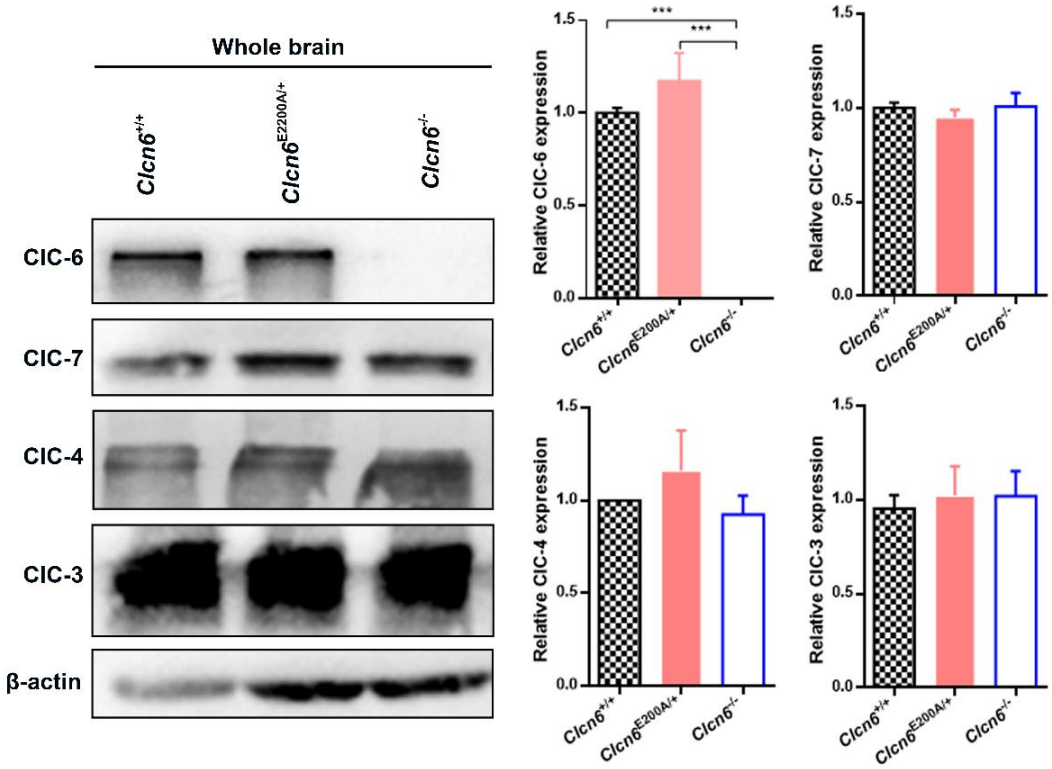

Figure S21 Protein levels of vesicular CLCs in mice at postnatal day 0 (P0). Quantification of Western blot analysis showed no change of ClC-6, ClC-7, ClC-4 and ClC-3 in the total brain extracts of *Clcn6*$^{E200A/+}$ mice, compared to WT littermates at P0. *Clcn6*$^{-/-}$ mice are used for comparison. Data were analyzed by one-way ANOVA with Tukey's multiple-comparison test for $n \geq 3$ per genotype and presented as mean ± SEM, ***$p < 0.001$.

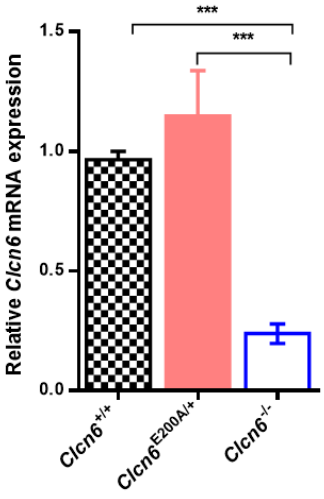

Figure S22 *Clcn6* mRNA levels in brain tissues at P0. qRT-PCR analysis revealed there was no significant difference in *Clcn6* mRNA levels of brain tissues between *Clcn6*$^{E200A/+}$ and WT mice at P0. As expected, *Clcn6* mRNA was not significantly decreased in brain tissues of *Clcn6*$^{-/-}$ mice. The relative expression of *Clcn6* was normalized to *Gapdh*. Data were analyzed by one-way ANOVA with Tukey's multiple-comparison test for $n \geq 3$ per genotype and presented as mean ± SEM, ***$p < 0.001$.

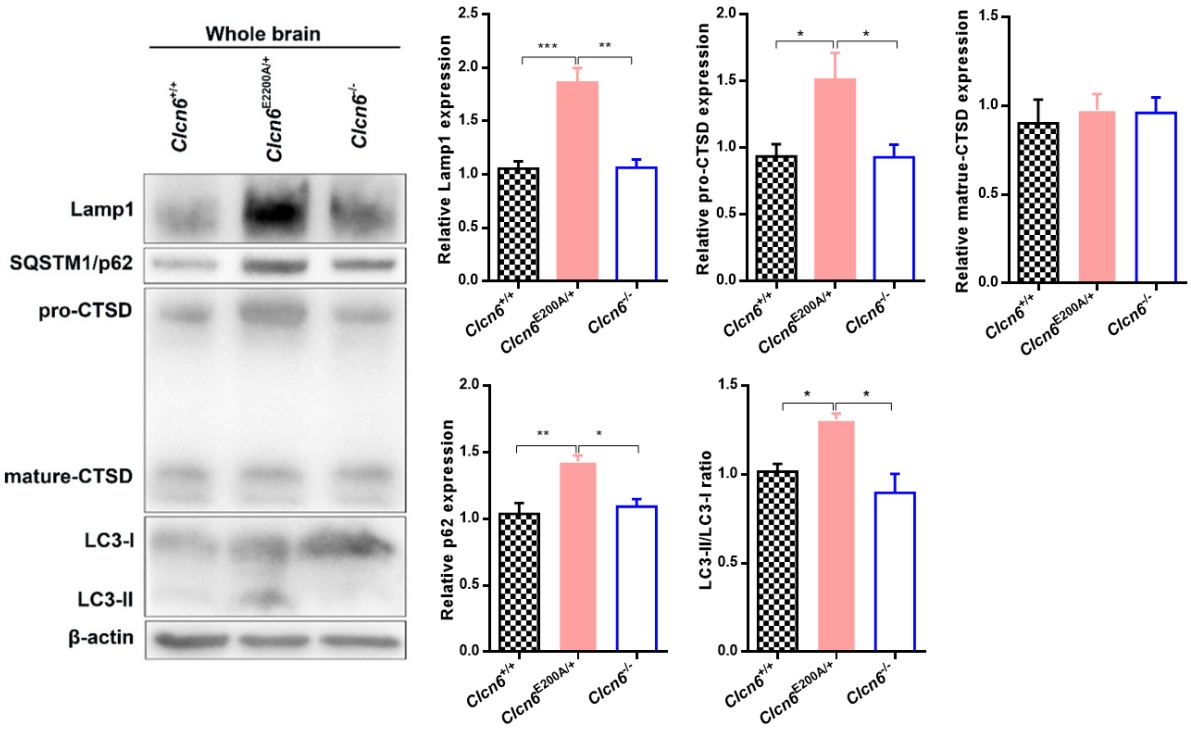

Figure S23 Lysosomal and autophagic protein levels in P35 mice. Western blot analysis showed an increase of Lamp1, SQSTM1/p62, pro-CTSD and LC3-II/ LC3-I in the total brain extracts of *Clcn6*$^{E200A/+}$ mice at P35, compared to age-matched WT or *Clcn6*$^{-/-}$ mice. β-actin was used for normalization. Data were analyzed by one-way ANOVA or nonparametric with Tukey's multiple-comparison test for n ≥ 3 per genotype per genotype and presented as mean ± SEM, *p < 0.05, **p < 0.01, ***p < 0.001.

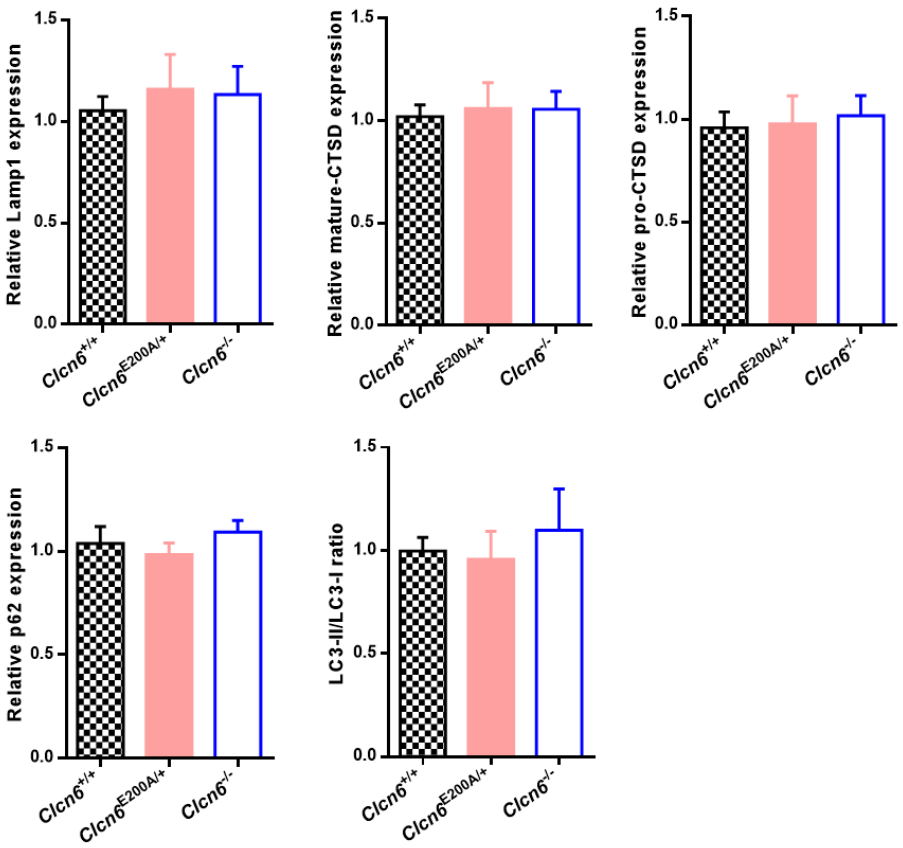

Figure S24 Lysosomal and autophagic protein levels in P0 mice. Quantification of Western blot analysis (as in Figure 7B) showed no change of ClC-6, Lamp1, SQSTM1/p62, pro-CTSD, mature-CTSD and LC3-II/ LC3-I in the total brain extracts of *Clcn6*$^{E200A/+}$ mice, compared to WT littermates at postnatal day P0. *Clcn6*$^{-/-}$ mice are used for comparison. All data were analyzed by one-way ANOVA or nonparametric with Tukey's multiple-comparison test for n ≥ 3 per genotype and presented as mean ± SEM.

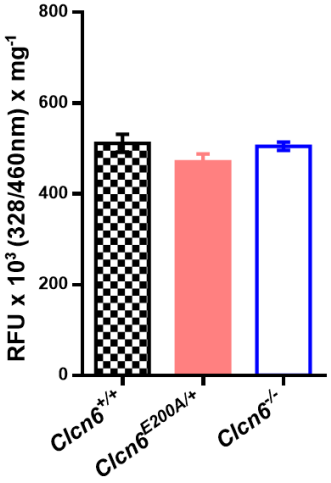

Figure S25 Cathepsin D (CTSD) in vitro enzyme activity assays. There was no measurable change in CTSD activity in the cortex of WT, *Clcn6*$^{E200A/+}$ and *Clcn6*$^{-/-}$ mice at 5 months. RFU: relative fluorescence units per microgram protein. Data were analyzed by one-way ANOVA with Tukey's multiple-comparison test for n ≥ 3 per genotype and presented as mean ± SEM.

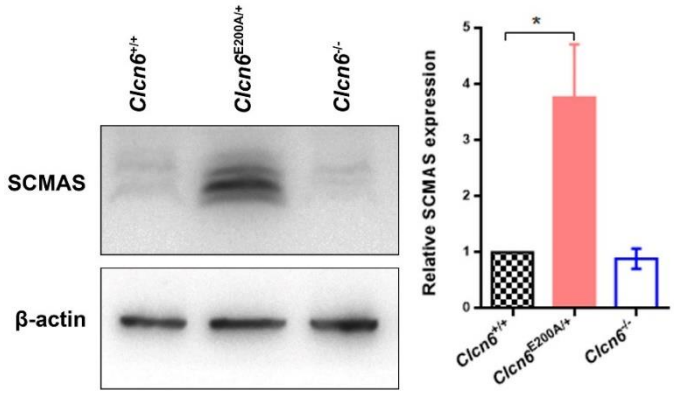

Figure S26 Protein levels of subunit c of the mitochondrial ATPase (SCMAS) in 5-month-old mice. Western blot analysis showed an increase in SCMAS levels in total brain extracts of *Clcn6*$^{E200A/+}$ mice at 5 months, compared to age-matched WT or *Clcn6*$^{-/-}$ mice. β-actin was used for normalization. Data were analyzed by nonparametric with Tukey's multiple-comparison test for $n \geq 3$ per genotype and presented as mean ± SEM, *$p < 0.05$.

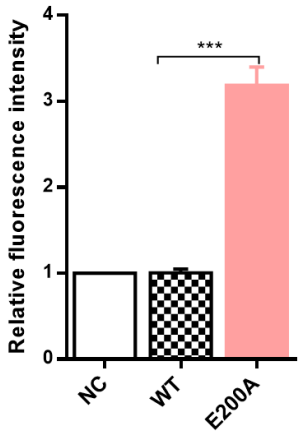

Figure S27 LysoTracker Deep Red staining. Total fluorescent intensity of LysoTracker signal (as in Figure 8B) in ClC-6 p.E200A-expressing cells is increased compared with ClC-6 WT-expressing cells. Values represent mean ± SEM of four independent experiments, one-way ANOVA with Tukey's multiple-comparison test, ***$p < 0.001$.

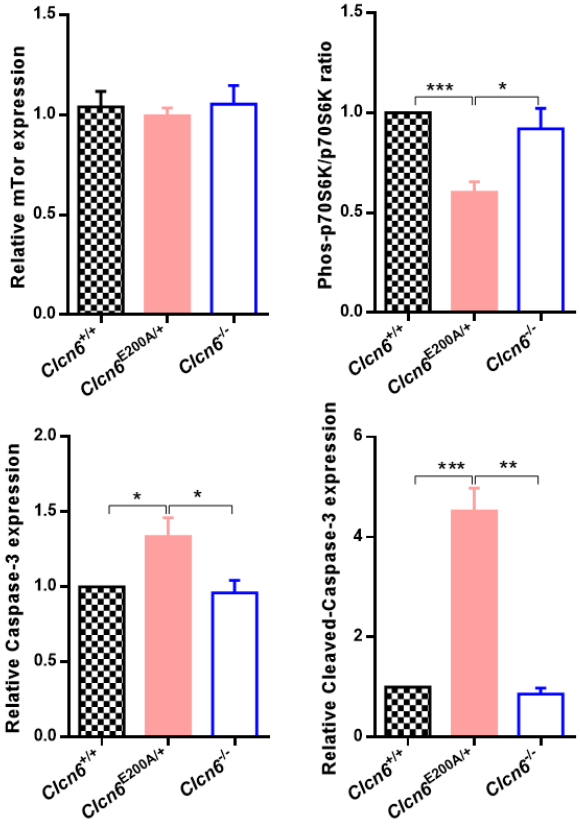

Figure S28 Western blot analysis of mTOR, phos-p70S6K, p70S6K, Caspase-3 and Cleaved-Caspase-3 in P35 mice in 4-month-old mice. Quantification of Western blot analysis (as in Figure 8C) of mTOR, phos-p70S6K, p70S6K, Caspase-3 and Cleaved-Caspase-3 in 4-month-old mice showed a decrease of phos-p70S6K/p70S6K, and an increase of Caspase-3 and Cleaved-Caspase-3 in total brain extracts of *Clcn6*$^{E200A/+}$ mice, compared to age-matched WT or *Clcn6*$^{-/-}$ mice. β-actin was used for normalization. Data are expressed as mean ± SEM for n ≥ 3 mice and were analyzed by one-way ANOVA or nonparametric with Tukey's multiple-comparison test. *p < 0.05, **p < 0.01, ***p < 0.001.

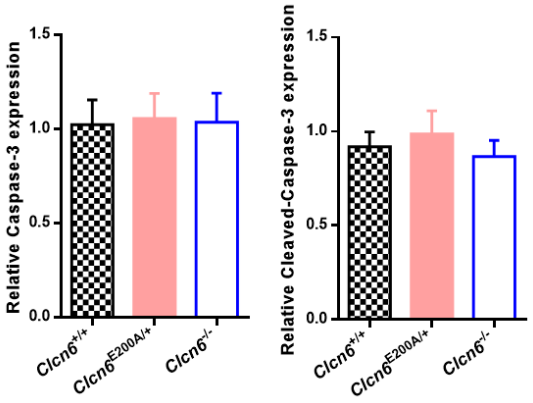

Figure S29 Western blot analysis of Caspase-3 and Cleaved-Caspase-3 in P35 mice. Quantification of Western blot analysis (as in Figure 8D) of Caspase-3 and Cleaved-Caspase-3 in P35 mice showed no change of Caspase-3 and Cleaved-Caspase-3 in total brain extracts of *Clcn6*$^{E200A/+}$ mice at P35, compared to age-matched WT or *Clcn6*$^{-/-}$ mice. β-actin was used for normalization. Data are expressed as mean ± SEM for n ≥ 3 mice and were analyzed by one-way ANOVA with Tukey's multiple-comparison test.

Supplemental movies

Movie S1: Tremor of a 4-month-old *Clcn6*$^{E200A/+}$ mouse.

Movie S2: Abnormal hunched gait with feet pointed outwardly and splayed hind limbs, and ataxia of a 5-month-old *Clcn6*$^{E200A/+}$ mouse.

Movie S3: The 5-month-old *Clcn6*$^{E200A/+}$ mouse in front had tonic-clonic seizures, followed by three consecutive head nodding seizures.

Movie S4: The 5-month-old *Clcn6*$^{E200A/+}$ mouse falls due to seizures accompanied by epileptiform discharges at the same time.

Movie S5: The 5-month-old *Clcn6*$^{E200A/+}$ mouse fell several times while trying to eat, followed by tonic seizures and abnormal circular movement, accompanied by epileptiform discharges at the same time.

Movie S6: The 5-month-old *Clcn6*$^{E200A/+}$ mouse had tonic seizures, accompanied by epileptiform discharges at the same time.

Supplemental tables

Table S1 Phenotypes and genotype characteristics associated with mutations in *CLCN6*

	Case1	Case2	Case3	Case4	Case5	Case6
Variant (NM_001286.3)	c.599A>C, p.E200A	c.599A>C, p.E200A	c.1658A>G, p.Y553C	c.1658A>G, p.Y553C	c.1658A>G, p.Y553C	c.1558A>G, p.T520A
Heterozygosity	Heterozygous	Heterozygous	Heterozygous	Heterozygous	Heterozygous	Heterozygous
Exon	Exon 8	Exon 8	Exon 16	Exon 16	Exon 16	Exon 16
Inheritance	*De novo*	*De novo*	*De novo*	*De novo*	*De novo*	*De novo*
Location in protein	Gating glutamate	Gating glutamate	Transmembrane helix Q	Transmembrane helix Q	Transmembrane helix Q	Transmembrane helix O
Ethnic background	Chinese	Chinese	European	European	European	South-American
Age	10 y, alive	10 y, alive	6 y 4 m, alive	23 m, deceased	18 m, alive	6 y 3 m, alive
Sex	Female	Male	Male	Female	Female	Female
Developmental delay / intellectual disability	Severe intellectual disability with regression	Severe intellectual disability with regression	Severe developmental delay with regression	Global developmental delay with regression	Global developmental delay with regression	Global developmental delay with regression
Seizures	Yes	Yes	No	No	No	Yes
Muscular tone	Generalized hypotonia	Lower limb hypertonia	Generalized hypotonia	Severe truncal hypotonia	Generalized hypotonia	Generalized hypotonia
Behavior problems	Autistic behaviors	Autistic behaviors	Not reported	Not reported	Not reported	Not reported
Visual impairment	Yes	Yes	Yes	Yes	Yes	Yes
Visual evoked potentials	Increased latency of P100 wave	No effective waveform in both eyes after multiple light stimulations	Increased latency and abnormal morphology of P100 wave	Not assessed	Not assessed	Deterioration of cortical visual responses with low amplitudes
EEG features	Bilateral sharp waves, spike waves, sharp and slow wave complexes, spike and slow wave complexes in bilateral frontal pole, frontal, anterior temporal region (10 y)	Hypsarrhythmia (8 m)	Frontal epileptic abnormallities (5 m).	Loss of normal background activity and structure with frequency slowing, no epileptic discharges (20 m)	Video EEG x2 negative (7 m)	Focal left temporo-central spike-and-wave Discharges (5 y)
Brain MRI	Progressive cerebellar and cerebral atrophy co-occurring with enlargement of the lateral ventricles	Frontal lobe dysplasia, thinned corpus callosum, and white matter T2-hyperintense signal (8 m)	Progressive cortical atrophy and bilateral brainstem lesions	Mild cerebral atrophy and brainstem lesions (18m)	Bilateral diffusion restriction in the cerebral peduncles and periaqueductal region (7 m and 22 m)	T2 hyper-intensity from the pons of the brainstem to the C6 vertebra (16 m)
Functional investigation	*In vitro* cell experiments, mouse experiments	*In vitro* cell experiments, mouse experiments	*In vitro* cell experiments	*In vitro* cell experiments	*In vitro* cell experiments	*In vitro* cell experiments
Functional effect	Gain of function	Gain of function	Gain of function	Gain of function	Gain of function	Gain of function
Reference	This study	He *et al.*[11]	Polovitskaya *et al.*[6]	Polovitskaya *et al.*[6]	Polovitskaya *et al.*[6]	Zhang *et al.*[12]

Table S2 Phenotypes of *Clcn6*$^{E200A/+}$ and *Clcn6*$^{-/-}$ mice

Neuropathological features	*Clcn6*$^{E200A/+}$	*Clcn6*$^{-/-}$
limb-clasping reflexes	+	-
vision impairment	+	+
motor and cognitive function deterioration	+	-
ataxia	+	-
seizures	+	-
early death	+	-
cerebral and cerebellar atrophy	+	-
enlargement of ventricles	+	+
accumulation of autofluorescent lipofuscin	+	+
accumulation of lysosomes, autophagosomes intracellular inclusion bodies, damaged organelles	+	-
Accumulation of SCMAS	+	+
progressive neuron loss	+	-
defective myelination	+	+
retinal neuron loss	-	-
microgliosis and astrogliosis	+	-

Table S3 Off-target primers

	Primer name	Primer sequence 5'- 3'	PCR product length
Site 1	Forward 1	AGATGTGCTAAACCAGAGACCTCC	545 bp
	Reverse 1	TAGGAAGTAAACAGGACCTGACAAG	
Site 2	Forward 2	AGTTTCTTCCAAGGGCTTTCTGC	551 bp
	Reverse 2	TTTAAGAGGAGGTCAGACGCTGC	
Site 3	Forward 3	TGGCTATCTTCTACTCCCATGATC	572 bp
	Reverse 3	TATTTACTGCCTCCTGCTGAGTTC	
Site 4	Forward 4	AGGAATTATCATTGCACTTTCAAGC	509 bp
	Reverse 4	AACCCTGTTAATCAACAAACAGGC	
Site 5	Forward 5	AGCCTGCAACTGTCGAACATTTG	575 bp
	Reverse 5	ATTTCCAGTTCACTTTCTGCTCCG	

Table S4 Primers used for qRT-PCR

Primer	Sequence (5'-3')	Nucleotides
Ctsa-F	CCCTCTTTCCGGCAATACTCC	22
Ctsa -R	CGGGGCTGTTCTTTGGGTC	19
Ctsb-F	TCCTTGATCCTTCTTTCTTGCC	22
Ctsb-R	ACAGTGCCACACAGCTTCTTC	21
Ctsd-F	GCTTCCGGTCTTTGACAACCT	21
Ctsd -R	CACCAAGCATTAGTTCTCCTCC	23
Ctsf-F	CCCTGGAAGCCACACTAGAG	21
Ctsf-R	GGGCTACAGTCCCTCCTCAG	20
Clcn7-F	CGCCAGTCTCATTCTGCACT	20
Clcn7-R	GCTTCTCGTTGTGTGGAATCT	21
Lamp1-F	CAGCACTCTTTGAGGTGAAAAAC	23
Lamp1-R	ACGATCTGAGAACCATTCGCA	21
Cln3-F	CCCTCGGTTGGATAGTCGGA	21
Cln3-R	GCCTGGTTCCACATGGCTC	19
Atp6v1h-F	GGATGCTGCTGTCCCAACTAA	21
Atp6v1h-R	TCTCTTGCTTGTCCTCGGAAC	21
Vps8-F	CCTCGTCTCAGGTAAAAATGTCG	23
Vps8-R	CACCTCGGTTCTGGGAGAG	19
Vps11-F	AAAAGAGAGACGGTGGCAATC	21
Vps11-R	AGCCCAGTAACGGGATAGTTG	21
Wipi-F	AGGATAACACGTCCCTAGCTG	21
Wipi-R	TCTCTCCACAATGCAGACATCT	22
Uvrag-F	ACATCGCTGCTCGGAACATT	20
Uvrag-R	CTCCACGTCGGATTCAAGGAA	21
Lc3b-F	TTATAGAGCGATACAAGGGGGAG	23
Lc3b-R	CGCCGTCTGATTATCTTGATGAG	23
Sqstm1-F	AGGATGGGGACTTGGTTGC	19
Sqstm1-R	TCACAGATCACATTGGGGTGC	22
Clcn6-F	TGACCGCTGCATCAATGACC	20
Clcn6-R	CAATGGCGAACACCACCATC	20
Gapdh-F	TTCACCACCATGGAGAAGGC	20
Gapdh-R	GGCATGGACTGTGGTCATGA	20

References

[1] Kominami E, Ezaki J, Muno D, Ishido K, Ueno T, Wolfe LS. Specific storage of subunit c of mitochondrial ATP synthase in lysosomes of neuronal ceroid lipofuscinosis (Batten's disease). J Biochem **1992**, *111*,278-82.

[2] Stobrawa SM, Breiderhoff T, Takamori S, Engel D, Schweizer M, Zdebik AA, Bösl MR, Ruether K, Jahn H, Draguhn A, Jahn R, Jentsch TJ. Disruption of ClC-3, a chloride channel expressed on synaptic vesicles, leads to a loss of the hippocampus. Neuron **2001**, *29*,185-96.

[3] Maritzen T, Keating DJ, Neagoe I, Zdebik AA, Jentsch TJ. Role of the vesicular chloride transporter ClC-3 in neuroendocrine tissue. J Neurosci **2008**, *28*,10587-98.

[4] Poët M, Kornak U, Schweizer M, Zdebik AA, Scheel O, Hoelter S, Wurst W, Schmitt A, Fuhrmann JC, Planells-Cases R, Mole SE, Hübner CA, Jentsch TJ. Lysosomal storage disease upon disruption of the neuronal chloride transport protein ClC-6. Proc Natl Acad Sci U S A **2006**, *103*,13854-9.

[5] Kornak U, Kasper D, Bösl MR, Kaiser E, Schweizer M, Schulz A, Friedrich W, Delling G, Jentsch TJ. Loss of the ClC-7 chloride channel leads to osteopetrosis in mice and man. Cell **2001**, *104*,205-15.

[6] Polovitskaya MM, Barbini C, Martinelli D, Harms FL, Cole FS, Calligari P, Bocchinfuso G, Stella L, Ciolfi A, Niceta M, Rizza T, Shinawi M, Sisco K, Johannsen J, Denecke J, Carrozzo R, Wegner DJ, Kutsche K, Tartaglia M, Jentsch TJ. A Recurrent gain-of-function mutation in *CLCN6*, encoding the ClC-6 Cl^-/H^+-exchanger, causes early-onset neurodegeneration. Am J Hum Genet **2020**, *107*,1062-77.

[7] Neagoe I, Stauber T, Fidzinski P, Bergsdorf EY, Jentsch TJ. The late endosomal ClC-6 mediates proton/chloride countertransport in heterologous plasma membrane expression. J Biol Chem **2010**, *285*,21689-97.

[8] Bárez-López S, Bosch-García D, Gómez-Andrés D, Pulido-Valdeolivas I, Montero-Pedrazuela A, Obregon MJ, Guadaño-Ferraz A. Abnormal motor phenotype at adult stages in mice lacking type 2 deiodinase. PLoS One **2014**, *9*,e103857.

[9] Pépin J, Francelle L, Carrillo-de Sauvage MA, de Longprez L, Gipchtein P, Cambon K, Valette J, Brouillet E, Flament J. In vivo imaging of brain glutamate defects in a knock-in mouse model of Huntington's disease. Neuroimage **2016**, *139*,53-64.

[10] Bouhy D, Juneja M, Katona I, Holmgren A, Asselbergh B, De Winter V, Hochepied T, Goossens S, Haigh JJ, Libert C, Ceuterick-de Groote C, Irobi J, Weis J, Timmerman V. A knock-in/knock-out mouse model of HSPB8-associated distal hereditary motor neuropathy and myopathy reveals toxic gain-of-function of mutant Hspb8. Acta Neuropathol **2018**, *135*,131-48.

[11] He H, Cao X, Yin F, Wu T, Stauber T, Peng J. West syndrome Ccaused by a chloride/proton exchange-uncoupling *CLCN6* mutation related to autophagic-lysosomal dysfunction. Mol Neurobiol **2021**, *58*,2990-9.

[12] Zhang B, Zhang S, Polovitskaya MM, Yi J, Ye B, Li R, Huang X, Yin J, Neuens S, Balfroid T, Soblet J, Vens D, Aeby A, Li X, Cai J, Song Y, Li Y, Tartaglia M, Li Y, Jentsch TJ, Yang M, Liu Z. Molecular basis of ClC-6 function and its impairment in human disease. Sci Adv **2023**, *9*,eadg4479.